RSC Advances

REVIEW

View Article Online
View Journal | View Issue

Cite this: *RSC Adv.*, 2025, **15**, 50233

Application of MOFs-mediated phototherapy in cancer treatment

Mengyu Xu,[a] Liyuan Wang,[c] Yuanxin Chen,[ab] Lihua Ma,[a] Min Liu,[a] Long Wang,[a] Jing Huan,*[d] Lijuan Wang*[a] and Yanxi Zhu *[a]

This article systematically discusses the latest progress of metal–organic frameworks (MOFs) in the field of cancer phototherapy. MOFs have overcome the limitations of conventional materials in structural design and functional tunability, offering ultra-high specific surface area, high porosity, and customizable active sites, which render them highly suitable as nanocarriers. In photodynamic therapy (PDT), MOFs can significantly improve the efficiency of ROS generation by loading photosensitizers or directly as photosensitive materials, and enhance tumour specificity by targeted modifications. In the field of photothermal therapy (PTT), MOFs have shown excellent near-infrared light absorption and conversion ability by integrating precious metal nanoparticles or designing novel ligand systems. It is worth noting that MOFs-mediated multimodal treatment strategies are increasingly mature. These innovations provide an important theoretical basis and technical path for the development of high-efficiency and low-toxicity nano-phototherapy systems.

Received 9th October 2025
Accepted 20th November 2025

DOI: 10.1039/d5ra07701j

rsc.li/rsc-advances

1. Introduction

Cancer is the second most common cause of death after cardiovascular disease and poses a significant threat to human well-being. The traditional treatments for cancer include radiotherapy, surgery, and chemotherapy. Unfortunately, these traditional treatment methods have shown many disadvantages. For example, chemotherapy has the problem of drug resistance, and the side effects of chemotherapy involve multiple systems and organs. As an invasive treatment, surgical treatment has some problems, such as surgical incisions. Radiotherapy kills not only tumor cells, but also normal cells, causing side effects. Chemotherapy, as the main treatment for cancer, has a great impact on its side effects and long-term sequelae.[1] Chemotherapy drugs lack the ability to distinguish between healthy cells and cancer cells, so they can also damage normal cells during treatment, leading to many adverse side effects in patients. In addition, most chemotherapeutic agents have poor pharmacokinetic profiles and require high doses and frequent administration to maintain therapeutic levels at the target site, both of which can increase adverse effects. Platinum-based chemotherapy is common in cancers. Experiments have shown that cisplatin causes changes in the endothelium of blood vessels at low doses and affects the function of the heart at high doses.[2] Therefore, compared with traditional treatment methods, it is a major topic to explore a treatment method that can not only improve the treatment efficiency but also produce fewer side effects. In this context, phototherapy has attracted attention as an alternative therapy with fewer side effects. Phototherapy (PT) can be traced back to 1903, when Niels Ryberg Finsen was awarded the Nobel Prize in Physiology or Medicine for his use of light to treat lupus vulgaris, regarded as the beginning of modern phototherapy.[3] PT is a minimally invasive and highly selective treatment. In recent years, PT has been widely used in the research of skin diseases and cancer treatment, because it kills tumor cells while causing less damage to normal tissues.[4] Phototherapy mainly includes photodynamic therapy (PDT) and photothermal therapy (PTT).[5] PDT is a minimally invasive therapy that relies on the effective positioning of photosensitizers for light irradiation and precise ablation of tumors.[6] In cancer treatment, after the enrichment of photosensitizer at the tumor site, local laser irradiation of the tumor site can selectively kill the tumor tissue and minimize the collateral damage to the surrounding normal tissues, which shows the great advantages of PDT in tumor treatment.[7] The main mechanism of PDT is to produce a large amount of Reactive Oxygen Species (ROS) to kill tumor cells.[8] PTT is also a relatively new minimally invasive and efficient tumor treatment method. It uses near-infrared light (NIR) and other light sources to irradiate the photothermal converting agent (PTCA)

[a]*Central Laboratory, Linyi People's Hospital, School of Clinical Medicine, Shandong Second Medical University, Shandong, China. E-mail: wanglj730@163.com; zhu-yanxi@163.com*

[b]*Tianjin Medical University Cancer Institute and Hospital, National Clinical Research Center for Cancer, Key Laboratory of Cancer Prevention and Therapy, Tianjin's Clinical Research Center for Cancer, Tianjin 300060, China*

[c]*Postgraduate Training Base of Linyi People's Hospital, Guangzhou University of Chinese Medicine, Linyi, China*

[d]*Department of Traditional Chinese Medicine, Linyi People's Hospital, Linyi, Shandong 276000, China. E-mail: 562625718@qq.com*

in the tumor area.[9] PTCA converts light energy into heat energy to kill tumor cells, because cancer cells are more sensitive to high temperature than normal cells.[10] The advantages of PTCA are short treatment time, high treatment efficiency, less side effects, and less trauma. Although phototherapy has many advantages, it still has disadvantages that cannot be ignored. Due to the limited penetration ability of light in tissues, it can only penetrate the skin or superficial tissues, so it is mainly suitable for superficial or near-surface tumors.[11] For deep tumors or metastatic tumors, its therapeutic effect is limited. In PDT treatment, severe pain and persistent photosensitivity cause discomfort to patients.[12] The photosensitizer in PDT therapy not only needs to be protected from light, but also its targeting and stability *in vivo* transportation need to be solved urgently.[13] The efficacy of PDT is highly oxygen dependent, but the tumor tissue is often in a hypoxic environment, and the therapeutic effect of PDT may be greatly reduced in a hypoxic environment.[14] In the treatment of PTT, PTCA also have the problems of low delivery efficiency and poor targeting. Moreover, PTT therapy is difficult to accurately control the generation and distribution of heat.[15] If the tumor treatment site is overheated, it will not only damage the surrounding normal cells, but also lead to heat shock response, triggering the host antitumor immunity, and some cells become heat tolerant, which will also lead to the reduction of the therapeutic effect.[16,17]

PDT has been used in the clinical treatment of tumors for more than 40 years, while PTT is generally used to enhance the local photothermal effect, which has not been widely carried out in clinical practice. Photosensitizers and PTCA play an important role, but are limited by the defects of traditional drugs, they are poor water solubility, poor photostability, and cannot be efficiently transported to the tumor site in the patient's body to play a phototherapeutic role.[13] Especially, photosensitizers are mostly hydrophobic molecules, easy to agglomerate into macromolecules, and are not easy to be transported to the lesion *in vivo*, so they cannot effectively play a tumor killing effect. It is urgent to construct a suitable nano-targeted drug delivery system to solve the above problems of traditional drugs. Compared with traditional nanocarriers (liposomes, inorganic nanoparticles, *etc.*), which have low drug loading, instability, and side effects. Metal–organic Frameworks (MOFs), as a relatively new porous crystal material, are porous hybrid materials composed of metal ions/clusters and organic linkers. In addition, MOFs can coordinate themselves into two-dimensional or three-dimensional network crystals.[18] MOFs have unique structural advantages in the construction of Nano Drug Delivery (nano-DDS):[19] (i) their controllable size, shape and good uniformity endow them with versatility; (ii) the large surface area and high porosity increase the loading of biomolecules and the encapsulation of various drugs; (iii) it has good biological safety and minimizes side effects; (iv) the internal properties of the surface are plastic, and its surface or interior can be modified, such as by selecting specific joints and metal clusters, choosing to change the surface area, morphology, hydrophilicity of the material, *etc.* These advantages not only avoid the problems existing in traditional nanomaterials, but also solve the defects of traditional phototherapy drugs. The metal ions can play a role in phototherapy, and the larger surface area to volume ratio can improve the drug loading efficiency and enhance the specific delivery (Fig. 1).

In this review, we discuss the mechanisms of PDT and PTT in cancer treatment, focus on and detail the research and progress of MOFs-mediated PDT, PTT, and their synergistic effect in cancer treatment, discuss the good prospects of their application in cancer treatment, and put forward a new prospect for the development of their potential clinical applications.

2. Mechanism of PT in cancer treatment

2.1 Mechanisms of PDT in cancer treatment

The three most important components in PDT are photosensitizer, light, and oxygen. In cancer treatment, photosensitizers are usually enriched in tumor tissues, and local irradiation of the tumor site by laser can selectively kill tumor tissues and minimize minor collateral damage to surrounding normal tissues[20] (Table 1). The main mechanism of PDT is to produce a large amount of ROS to kill tumor cells.[21] There are two main sources of ROS.[22] Type I reaction is that photosensitizers directly interact with neighboring biomolecules in cancer cells to produce free radical intermediates, and then interact with oxygen (O_2) to produce ROS, such as superoxide anion ($O_2^{-\bullet}$), hydroxyl radical ($^{\bullet}OH$), hydrogen peroxide (H_2O_2), *etc.* Type I reaction is the singlet oxygen ($^1O_2$) produced by the transfer of photosensitizers electron energy to the ground molecular oxygen.[23] Classical type II PDT has been extensively studied, and $^1O_2$ is believed to play an important role in PDT reactions.[24] Photosensitizers transfer the energy of photoexcitation to O_2 to generate $^1O_2$, which can cause oxidative damage to tumor cells. It can oxidize biological macromolecules such as proteins, lipids and nucleic acids to peroxide free radicals, which can cause oxidative damage to tumor cells.[25] Superoxide anions

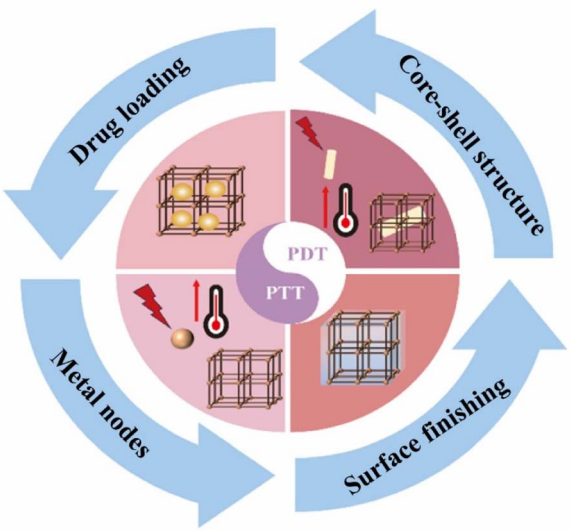

Fig. 1 Specific ways in which MOFs play a role in the phototherapy process.

Table 1 Photosensitizers that have been clinically approved or are currently in clinical trials

Product	Bases	Indications/uses	Ref.
Photofrin®	Hematoporphyrin	Skin cancer, esophageal cancer, lung cancer *etc.*	29
Levulan®	5-Amino ketoglutaric acid	Skin photodynamic therapy (basal cell carcinoma)	30
Metvix®/Hexvix®	Protoporphyrin IX	Photodynamic diagnosis of bladder cancer	31 and 32
Visudyne®	Verteporfin	Macular degeneration (photodynamic therapy)	33
Talaporfin (Laserphyrin)	Chlorine derivatives	Esophageal cancer, lung cancer	34
Temoporfin (Foscan)	Phthalocyanines	Head and neck cancer	35
Silicon phthalocyanine	Phthalocyanine-4	Skin/subcutaneous tumor	36
Redaporfin	Bacterial chlorine derivatives	Skin cancer, breast cancer	37
Phthalocyanine	Near-infrared dye (IR-700)	Targeted photothermal/photodynamic (antibody conjugated)	38

($O_2^{-\bullet}$) and hydroxyl radicals ($^\bullet OH$) play a major role in type I PDT. $^\bullet OH$ is a kind of ROS with strong oxidizing capacity and high activity, which can effectively kill tumor cells.[26] $^\bullet OH$ can be produced by oxidoreductases in addition to Fenton and Fenton-like reactions. $O_2^{-\bullet}$ can react with biomacromolecules or reducing substances in cells to regulate REDOX balance and control the expression of related substances, which is widely used in cancer treatment.[27] Compared with type II PDT, the research on type II PDT is less. Type I PDT has the problem of hypoxia tolerance, while type II PDT shows high reactivity.[28] Therefore, in biomedicine, the two reactions are often combined to produce reactive oxygen species.

The mechanism of PDT killing tumor cells is different, but many scholars generally agree that: (1) ROS targeted delivery to cancer cells promotes oxidative stress response, leading to the activation of protein kinase pathway, transcription factor and cytokine expression, and release of apoptosis-mediated factors, leading to cell apoptosis or necrosis;[39,40] (2) PDT can effectively target tumor blood vessels and indirectly kill cancer cells by destroying tumor vasculature and causing tumor ischemia;[41] (3) the acute local and systemic inflammatory response induced by PDT eventually stimulates the activation of T cells and generates anti-tumor immune response, further inhibiting tumor growth and recurrence.[42] However, the efficacy of PDT still faces two major challenges: one is the drug resistance of tumors, and the other is the limited efficiency of ROS generation.[43] This is mainly attributed to the poor solubility of photosensitizers in solid tumors, their tendency to aggregate, and the depletion of oxygen in the hypoxic microenvironment of tumors. To address these issues, MOFs have shown great potential. The structure and function of MOFs are highly tunable, and their highly porous framework not only allows ROS to diffuse rapidly but also effectively prevents the self-quenching phenomenon of photosensitizers. These characteristics make MOFs have very broad application prospects in enhancing the efficacy of PDT.[44]

2.2 Mechanisms of PTT in cancer treatment

PTT is a novel cancer treatment method that is simple to operate and leads to quick recovery for patients. Its core lies in the use of photothermal conversion agents (PTCA), which convert light energy into heat energy under the irradiation of external near-infrared light, precisely eliminating tumors. Near-infrared light is preferred as the light source for PTT due to its excellent tissue penetration and three-dimensional selectivity[45] (Table 2).

The therapeutic mechanism of PTT mainly stems from the local thermal effect. When PTCA accumulates at the tumor site, external irradiation can raise the local temperature to above 40 °C. This high-temperature environment directly damages the cancerous tissue and enhances the sensitivity of the tumor to radiotherapy or chemotherapy.[54,55] At the cellular level, the high temperature functions through the following pathways: on one hand, it directly destroys key biomolecules such as nucleic acids, liposomes, and proteins within the tumor cells; on the other hand, it can induce the production of cell cycle arrest proteins such as p53, further exacerbating the damage to these biomolecules, and ultimately triggering tumor cell apoptosis.[56,57] PTT can also activate anti-tumor immunity. Thermal therapy prompts the release of antigens, pro-inflammatory cytokines, and immunogenic substances from dead tumor cells, thereby stimulating a specific immune response and systematically eliminating the tumor.[58] Additionally, the thermal effect can damage tumor vasculature, resulting in reduced blood flow, thrombosis, and subsequent hypoxia and nutrient deprivation, thereby indirectly inducing tumor cell death.[59]

The key to the therapeutic effect of PTT is PTCA. The relative main characteristic of PTCA is the photothermal conversion efficiency.[60] PTCA is mainly divided into two categories: organic and inorganic. Inorganic materials mainly include precious metal materials (gold, silver, *etc.*), excessive metal sulfide (copper sulfide, *etc.*), carbon-based materials (graphene, *etc.*), and organic materials, including near-infrared fluorescent dyes (ICG, IR-820, *etc.*) and polymers.[61] So far, although the excited inorganic materials have good photothermal conversion efficiency and photostability, they all share a common drawback, such as poor biosafety and biodegradability, inducing immune response *in vivo*, and potential long-term toxicity, which have hindered their clinical application. Organic materials are highly biodegradable, less toxic, and structurally diverse. The efficacy of PTT may be limited by insufficient tumor vasculature if PTCA is used solely to enhance heat production. Due to their structural diversity and designability, MOFs materials can realize the absorption and conversion of light at different wavelengths by selecting different metal ions, organic ligands, or adjusting the

Table 2 Common PTCA in PTT treatment

Classification	Example	Advantage	Disadvantage	Ref.
Noble metal nanoparticles	AuNRs, AuNPs, silver, platinum, palladium *etc.*	Strong surface plasmon resonance (LSPR), high photothermal conversion efficiency, easy surface functionalization	High cost and long-term biological safety concerns	46
Carbon-based materials	Graphene, graphene oxide, carbon nanotubes, carbon quantum dots, black phosphorus (BP)	Large specific surface area, wide light absorption range; some materials have stronger absorption in the NIR-II region	The material is prone to aggregation and has poor long-term stability	47
MXene family	$Ti_3C_2T_x$, Nb_2CT_x *etc.*	Possess metallic-like high conductivity and strong NIR absorption, and photothermal efficiency can be enhanced through interlayer regulation	The spectral absorption range is limited, the preparation process is complex, the cost is high, and the stability in an oxygen/water environment is poor	48 and 49
MOFs derivatives	Pt/PCN-224(Zn), Pd@ZIF-8 *etc.*	Combining photothermal and photocatalytic dual functions, can achieve photothermal catalysis in organic transformations	Metal ion toxicity, scale-up challenges, and relatively low photothermal conversion efficiency	50
Small molecule dyes	Indocyanine green (ICG), Prussian blue, BODIPY, phthalocyanine, porphyrin, quinoline *etc.*	Absorption peaks located in the NIR-I region, structure can be adjusted to regulate photothermal conversion efficiency	Some dyes tend to aggregate in water and require carriers or polymer encapsulation	51
Conjugated polymers/ nanoparticles	Poly pyrrole (PPy), poly aniline (PANI), poly dopamine (PDA), semiconductor polymers (such as PPV, PDPP)	High photothermal conversion through non-radiative relaxation, good biocompatibility, and can be directly synthesized into nanoparticles or coatings	Easy to aggregate, low water solubility and poor biodegradability	52
Natural pigments	Melanin, heme derivatives, chlorophyll derivatives *etc.*	Natural sources, low toxicity	Photothermal efficiency is limited by molecular structure	53

synthesis conditions.[62] This property enables MOFs to be used as efficient PTCA. Despite the great advantages of PTT therapy, most of the current PTT therapies rely on non-degradable PTT agents, which may bring potential long-term and chronic toxic side effects to the organism. Therefore, the research on PTCA with high biological safety and metabolic decomposition is of great research value for further clinical research of nanomedicine-based materials.

PTT also has some limitations,[63] such as: (i) the penetration depth of light is limited, resulting in incomplete ablation of the tumor; (ii) thermal damage to the surrounding normal tissues during the treatment; (iii) PTT may induce heat shock response and host anti-tumor immunity. Therefore, the use of mild photothermal therapy to treat tumor diseases is a common pursuit. Whether by regulating the expression of heat shock proteins (HSP), the generation of ROS, or enhancing the sensitivity of cells to mild temperature increases, PTT therapy is more efficient and less damaging to normal tissues.[64] Cai *et al.* used the MoS_2 core to produce a low temperature of 40–48 °C, then modified it with DPA and loaded it with Fe^{2+}, then loaded it with CPT-11, and finally modified it with PEG and iRGD to enhance the tumor specificity.[65] Finally, the MoS_2/Fe@CPT-11-PEG-iRGD nanoplatform was synthesized. Experiments showed that NIR and tumor acidic conditions triggered the release of CPT-11 and Fe^{2+}. CPT-11 increased H_2O_2 and reacted with Fe^{2+} to produce lipid ROS, destroy mitochondria, and degrade HSP70/90 protein. The results showed that the combination of chemotherapy, ferroptosis, and low-temperature PTT exerted an excellent tumor-killing effect, which provided an idea for the clinical application of low-temperature photothermal therapy and opened up a potential path for the combined treatment of tumors by multiple mechanisms. Due to the special characteristics of MOFs, including high porosity, large surface area, large pore size, nanometer size, biocompatibility, and biodegradability, they have great potential in biomedical applications. In order to solve the above problems, the nano-targeted drug delivery system constructed by MOFs can change the basic characteristics and biological activity of drugs, stay in the blood circulation for a longer time, and ensure the controlled release of drugs in a specified space and time. Compared with larger particles (1–10 μm), nano-scale materials can be integrated into tissue systems to promote

cellular drug uptake, achieve effective targeted drug delivery, and ensure the effect at the target site.

3. MOFs and their classification

3.1 MOFs

MOFs is a class of hybrid porous materials composed of metal ions connected with organic ligands through coordination interaction.[66] The development of MOFs has gone through a long period of time and has been perfected step by step with the idea of scientists. In 1965, Tomic first reported a new solid material composed of carboxyl linkers and metal ions, and explored the relationship between the thermal stability of coordination polymers, the valence of metal ions and the coordination sites on the linkers, which was regarded as the prototype of MOFs.[67] In addition, Hoskins and Robson proposed a porous low-density infinite 3D framework and scaffold with high thermal and chemical stability based on the chemistry knowledge of coordination polymers in 1990.[68] All these studies laid the foundation for the discovery of MOFs. In 1995, Omar Yaghi of the University of California, Berkeley synthesized large-aperture 3D crystals $[Cu(I)(4,4'\text{-Bipy})_{1.5}\text{–}NO_3]\cdot(H_2O)_{1.25}$ and first proposed the term "MOFs".[69] In 1997, Kitagawa in Japan first demonstrated the "porosity" of metal complexes through gas adsorption experiments.[70] However, the pore size and stability of the materials were limited, which also limited the biomedical applications. In 1999, Yaghi and his team reported a 3D open-skeleton MOF-5 (also known as IRMOF-1), copper-based MOF with benzene tricarboxylate linker.[71] Removing the guest molecules in the pore channel can still keep the skeleton intact, and the pore size can be controlled, which makes it widely used in gas adsorption, catalysis, drug delivery, and other fields. Due to their unique porous architecture, MOFs can efficiently encapsulate therapeutic agents within a short time frame, rendering them highly promising candidates for drug delivery applications.[72] Taking ZIF-8 as an example, the Zn^{2+} ions and imidazole-based ligands exhibit a propensity for protonation under acidic conditions, which facilitates rapid structural disintegration and drug release in the tumor microenvironment (pH $\approx$ 6.5), thereby significantly enhancing intracellular drug efficacy. By incorporating photoresponsive moieties—such as porphyrins or photosensitive metal complexes—into the organic ligands or metal nodes, light-responsive DDS can be engineered. Upon light irradiation, these systems enable spatiotemporally controlled drug release while simultaneously generating reactive oxygen species for PDT. Notably, certain metal nodes—such as Fe^{3+}, Al^{3+}, Zr^{4+}, and Hf^{4+}—exhibit inherently low biotoxicity. When co-loaded with drugs at the nanoscale, the overall system can maintain toxicity within a safe physiological range, further broadening the biomedical applicability of MOFs.

With the progress of science and technology, scientists have put MOFs in the application of nanomedicine. The first MOFs material to enter the human clinical trial stage is RiMO-301, developed by Wenbin Lin's team at the University of Chicago.[73] RiMO-301 is composed of a proprietary X-ray absorbing metal that can absorb X-ray photons and generate ROS, inducing ROS-mediated DNA damage in irradiated cancer cells, thereby leading to tumor cell lysis.

3.2 Classification of MOFs

MOFs is also a kind of porous material with a fast expansion rate and a wide variety. More than 90 000 MOFs structure have been reported so far.[74] Different MOFs is held together by fragile coordination bonds between different connectors and metal clusters, which not only determine their versatile structures and characteristics, but also enhance biodegradability. Therefore, selecting appropriate metal ions and organic ligands for binding can ensure good stability and biodegrade ability of the materials.[75] In terms of biosafety, the biocompatibility and toxicity of synthetic MOFs had better be predictable.[76] Then the toxicity of metal is particularly important, which mainly depends on the type, oxidation state, and dose.[77] The median lethal dose (LD_{50}) is commonly used to assess metal toxicity. In addition, recommended metal clusters as materials for MOFs are potassium, zinc, zirconia, and iron, with oral LD_{50} of 0.215, 0.35, 4.1, and 0.45 g kg^{-1}, respectively.[78,79] There are many types of MOFs, and the classification methods are varied. This article focuses on the classification of MOFs according to the different metal ions that compose them.

3.2.1 Cr-MOFs. Cr-MOFs have attracted attention because of their better chemical stability. MIL-100(Cr) was first developed by the FeRey research group of the University of Versailles in France.[80] It was first synthesized and reported in 2004. It is a hypertetrahedron formed by the connection of Cr with the organic ligand triphenyl acid (1,3,5-BTC) as a secondary structural unit, and its thermal stability can reach 270 °C. The initial synthesis time of the MIL-100 framework is 96 hours, which greatly hinders its practical application. Until 2005, Jhung *et al.*, for the first time, began to synthesize MOFs by microwave radiation method, and the synthesis was MIL-100(Cr), which shortened the time from 96 h to 4 h and improved the synthesis efficiency.[81] In the same year, MIL-101(Cr) was first reported by Ferey *et al.*, which is a kind of chromium phthalate MOFs.[82] MIL-101(Cr) has excellent hydrothermal/chemical stability and can maintain structural stability at 275 °C.[83] Another high-connected chromium MOFs also has good chemical stability, which can withstand extreme conditions from pH < 0 or pH > 14.[84] The good stability lays a good foundation for the biological application of Cr-MOFs, but the toxicity of Cr is relatively high, and its biological safety is not ideal (Fig. 2A).

3.2.2 Fe-MOFs. Fe-MOFs have great potential in the field of nanomedicine due to their low toxicity, adjustable degradability, and structural versatility. MIL-53(Fe) is an early product of Fe-MOFs, which is composed of Fe(III) octahedra and terylene acid or its derivatives. It has a highly ordered pore structure and large surface area, making it a great potential in gas adsorption, separation, and catalysis.[90,91] The initial generation of MOFs has micropores (<2 nm), which seriously limit their drug loading efficiency and affect their application in medical therapy.[92] MIL-100(Fe) and MIL-101(Fe) were successfully prepared by other researchers on the basis of MIL-100(Cr) and MIL-101(Cr) synthesized by Ferey's team through the replacement of metal

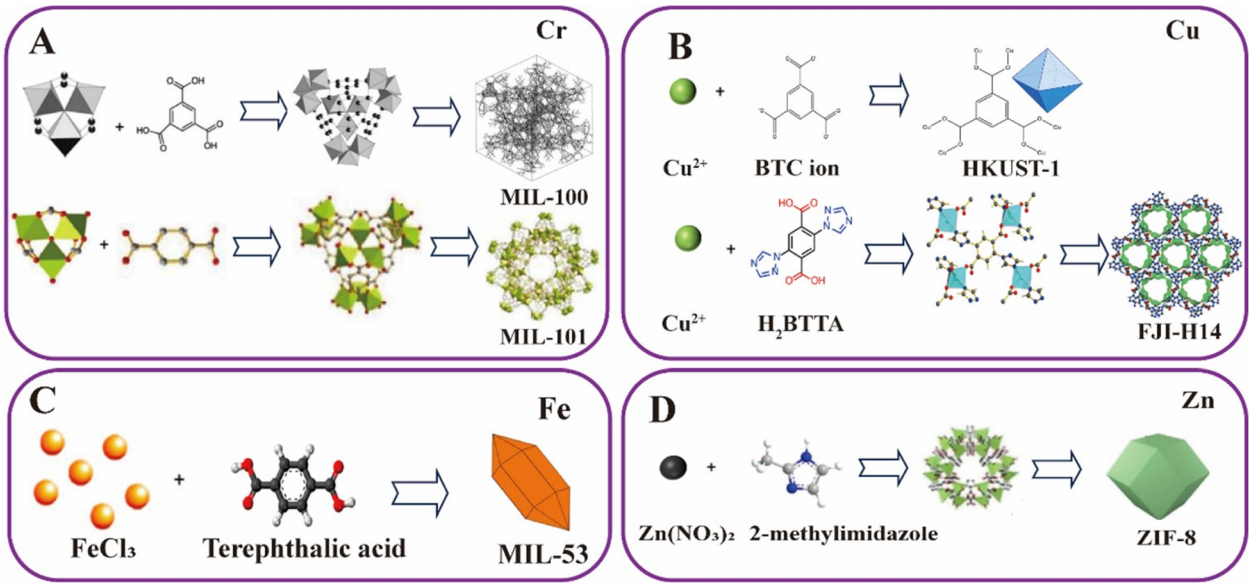

Fig. 2 (A) Synthesis of MIL-100(Cr)[53] and MIL-101(Cr).[85] Panel (A) reproduced from ref. 53 with permission from John Wiley and Sons, copy 2004; reproduced from ref. 85 with permission from Elsevier, copy 2022. (B) Synthesis of HKUST-1 (ref. 86) and FJI-H14.[87] Reproduced under a Creative Commons CC BY Attribution 4.0 International License.[86,87] (C) Synthesis of MIL-53(Fe).[88] Panel (C) reproduced from ref. 88 with permission from Elsevier, copy 2022. (D) Synthesis of Zif-8.[89] Panel (D) reproduced from ref. 89 with permission from John Wiley and Sons, copy 2022.

elements, showing good pore size and surface area. Fe-MOF is actively used by scientists in the treatment of cancer. Studies have found that Fe(III) can not only act as a catalyst for Fenton reaction, which can convert H_2O_2 to O_2 at the tumor site, thereby regulating local hypoxia conditions; it can also be used as a T_1-weighted magnetic resonance imaging (MRI) contrast agent, allowing the monitoring of tumor treatment response, which has played a great role in the monitoring and treatment of tumors[93] (Fig. 2C).

3.2.3 Zr-MOFs. MOFs are named based on where they were found. Before 2008, stable boxes for other metals, such as Fe^{3+} and Cr^{3+} existed in the field of MOFs. UiO-66 was first reported by Jasmina and her team at the University of Oslo in 2008.[94] It is composed of a zirconium ion (Zr^{+}) and a dicarboxylic acid ligand. This kind of material is of great interest due to its relatively simple preparation method and excellent water and chemical stability. In 2011, Behrens' team introduced benzoic acid/acetic acid as a modulator, which not only increased the specific surface area of Zr-MOFs but also increased the degree of crystallinity.[95] Due to the excessive oxidation state of Zr(IV) in Zr-MOFs and the strong coordination bond between Zr(IV) and carboxylate ligands in the vast majority of carboxylate Zr-MOFs, they have unparalleled stability. Therefore, a large number of Zr-MOFs are not only stable in organic solvents and water, but also stable in the acidic environment of tumors.[75,96] Due to the advantages of good stability, low toxicity, and good biocompatibility, Zr-MOFs have shown good application prospects in the fields of drug delivery, photodynamic therapy, and fluorescence sensing.[97] They expect UiO-66 to have great potential in drug delivery, bioimaging, and other fields.

3.2.4 Cu-MOF. In 1995, Yaghi's team first proposed the term "MOFs" and reported the first copper-based coordination polymer $[Cu(I)(4,4'\text{-Bipy})_{1.5}\text{–}NO_3]\cdot(H_2O)_{25}$, which was proved to have non-permanent microporous channels and laid the foundation for the structural design of Cu-MOFs.[69] In 1999, the Chui team reported the synthesis of HKUST-1(also known as MOF-199 or $Cu_3(BTC)_2$) by the solvothermal method.[98] The material is mainly composed of copper clusters and organic ligands connected to each other to form a high-crystallinity three-dimensional porous network, which became a milestone for Cu-MOFs. HKUST-1 was first generated by electrochemical synthesis in 2005.[99] Compared with the traditional method, the specific surface area of the materials obtained by this method is increased. Copper is necessary for cancer growth and metastasis, so it plays an important role in anti-tumor.[100] Although Cu-MOFs have shown great potential in medical applications, their application *in vivo* still faces some challenges. For example, traditional Cu-MOFs are easily hydrolyzed, have instability, and copper ion toxicity problems. To solve this problem, Liang *et al.* demonstrated the design and synthesis of a Cu(II) MOFs (FIJ-H14) with a high density of active sites, and verified its acid-base stability and high-temperature resistance.[87] Experiments showed that FIJ-H14 was not only very stable in boiling water, but also very stable in acid and base environments from pH = 2 to pH = 12 and at temperatures up to 373 K (Fig. 2B).

3.2.5 Zn-MOFs. Zn-MOFs can be traced back to 1998, when Yaghi's team reported the first Zn-MOFs, MOF-2.[101] In 1999, Yaghi reported that MOF-5, a three-dimensional open MOFs with a simple cubic structure, was constructed with an organic ligand, terephthalic acid (BDC), and transition metal Zn.[71] MOF-

5 could be stable when solvent molecules were removed from the pore and heated to 300 °C. ZIF-8 is a representative Zn-MOFs material, which has made significant progress in the therapeutic application of cancer. Park's team first synthesized ZIF-8 by the solvothermal method in 2006.[102] Zif-8 is composed of zinc ions linked with 2-methylimidazole (H-MeIM), and its large pore size and excellent thermal stability were introduced by the authors. ZIF-8 is a kind of material widely used in biomedical applications, and the simplicity and safety of synthesis are particularly important in the application of materials. In 2011, Pan *et al.* proposed a new synthesis method to prepare ZIF-8 in aqueous solution at room temperature.[103] This method not only shortens the synthesis time but also solves the problem of solvent toxicity (Fig. 2D).

3.2.6 Hf-MOFs. Hf-MOFs possess unique chemical, thermal and mechanical stability, making them the most stable type of MOFs. Hf-MOFs were first reported in 2012. Scientists synthesized UiO-66(Hf) based on UiO-66(Zr), while maintaining the stability of the UiO-66 type MOFs. Generally speaking, by replacing Zr with Hf under similar conditions, MOFs similar to Zr-MOFs can be generated. Moreover, Hf-MOFs have higher stability because the Hf–OH stronger Brønsted acidic sites are stronger than those in Zr SBUs. Due to their stability, scientists have shown great enthusiasm for them, but the synthesis of Hf-MOFs is limited by the traditional homogeneous solvent heating process, which limits its practical application. He *et al.* accelerated the generation rate of UiO-66(Hf) by controlling the hydrolysis and nucleation of metal salts in the presence of acetic acid and water, thus paving the way for its practical application.[104] The Hf-MOFs was first proposed by the Lin team in 2014 in the research of PDT. It is used to load porphyrin substances, and has shown significant effects in the treatment of head and neck cancers.[105]

4. Application of MOFs in tumour PT

4.1 Application of MOFs in PDT

PDT uses light to irradiate photosensitizers in the presence of oxygen to damage or destroy living cells.[106] Over the past decades, numerous efforts have been made to address these limitations of PDT, many of which are aimed at improving two aspects of PDT: discovering or synthesizing more powerful photosensitizers and improving the localization of photosensitizers in tumors.[107] Allahloubi *et al.* endowed the photosensitizer with targeting ability to myeloma cells and achieved therapeutic effect.[108] The article showed that the photosensitizer reduced the survival rate of myeloma cells to 25% under laser irradiation. Zinc phthalocyanine is known for its high monomer oxygen generation in physiological media, mainly by exploiting the diamagnetism of zinc ions. MOFs are porous hybrid materials that are self-assembled by metal ions and organic ligands.[109] If the diamagnetic properties of metal ions are combined with the porosity of MOFs, it is possible to construct a nano-targeting system that can not only load chemotherapy drugs, but also perform the PDT function of MOFs.

In order to realize the very active role of MOFs in PDT, there are generally the following three methods: (i) in the most commonly used method, the photosensitizer is directly loaded into the pore size of MOFs through physical reaction, but this method has certain limitations. The loaded photosensitizer must be smaller than the pore size of MOFs, and this simple loading can easily lead to the leakage of photosensitizer during the delivery process; (ii) the photosensitizer can be chemically modified by combining with the surface active sites of MOFs, such as amino and carboxyl groups. However, not all MOFs have corresponding sites, which is not universal; (iii) functional molecules with photosensitizing properties are used as organic ligands or metal ions for the synthesis of MOFs, but this makes the synthesis step more complicated. Among them, the use of photosensitive functional molecules as part of the synthesis of MOFs is the most unique aspect of MOFs in the aspect of drug delivery. In the process of PDT, there is no release, and due to the highly porous structure of MOFs, ROS can quickly diffuse out of MOFs and play a direct and efficient PDT effect.[110] In the following, we will introduce the application of MOFs in photodynamic therapy according to the above three methods.

The first report of MOFs PDT appeared in 2014, when Lin's group first reported a Hf^{-} porphyrin MOFs, DBP-Hf, as an efficient photosensitizer for PDT in drug-resistant head and neck cancer[111] (Fig. 3A). DBP-Hf was synthesized in dimethylformamide (DMF) by the solvothermal method using Hf^{4+} as a metal ion and 5,15-bis(*p*-benzoic acid)porphyrin (H_2DBP) as an organic ligand. Among them, DBP molecules are separated by metal nodes to avoid aggregation and quenching, and the coordination of DBP molecules with Hf promotes energy transfer, thereby promoting the production of ROS.[112] Experiments show that DBP-Hf is at least twice as efficient as H_2DBP in producing $^1O_2$. Not only that, DBP-HF shows a nanosheet morphology with a diameter of about 100 nm and a thickness of about 10 nm, which facilitates $^1O_2$ diffusion. In the *in vivo* experiment, DBP-Hf treatment reduced tumor volume by 50-fold in half of the mice and completely eradicated tumors in the other half of the mice; free H_2DBP had no significant effect. Based on the powder X-ray diffraction (PXRD) pattern, DBP-Hf was considered to be a UIO-type MOFs structure, but it was later redesignated as a new HF-MOFs structure with Hf_{12} cluster secondary building units (SBUs).[113] Although DBP-Hf is effective, there is still room for optimization of its photophysical properties. Subsequently, in 2015, Lin's group reported the first chlorine-based MOFs.[114] The scientists used H_2DBC as a bridging ligand and Hf^{4+} as a metal ion to synthesize DBC-Hf, and demonstrated its application in cancer PDT. Compared to DBP-Hf reported by this group, DBC-Hf not only retains all the properties of DBP-Hf (crystal stable structure, prevention of self-quenching, $^1O_2$ generation efficiency is three times that of DBP-Hf), and the distance between adjacent (111) layers (d_{111}) is 2.2 nm, thinner nanoplates are more conducive to $^1O_2$ diffusion, it is also characterized by significantly enhanced photophysical properties. For example, DBC-Hf extends the absorption wavelength range closer to the near-infrared region (600–900 nm), enhancing tissue penetration; the extinction coefficient of DBC-Hf is 11 times higher than that

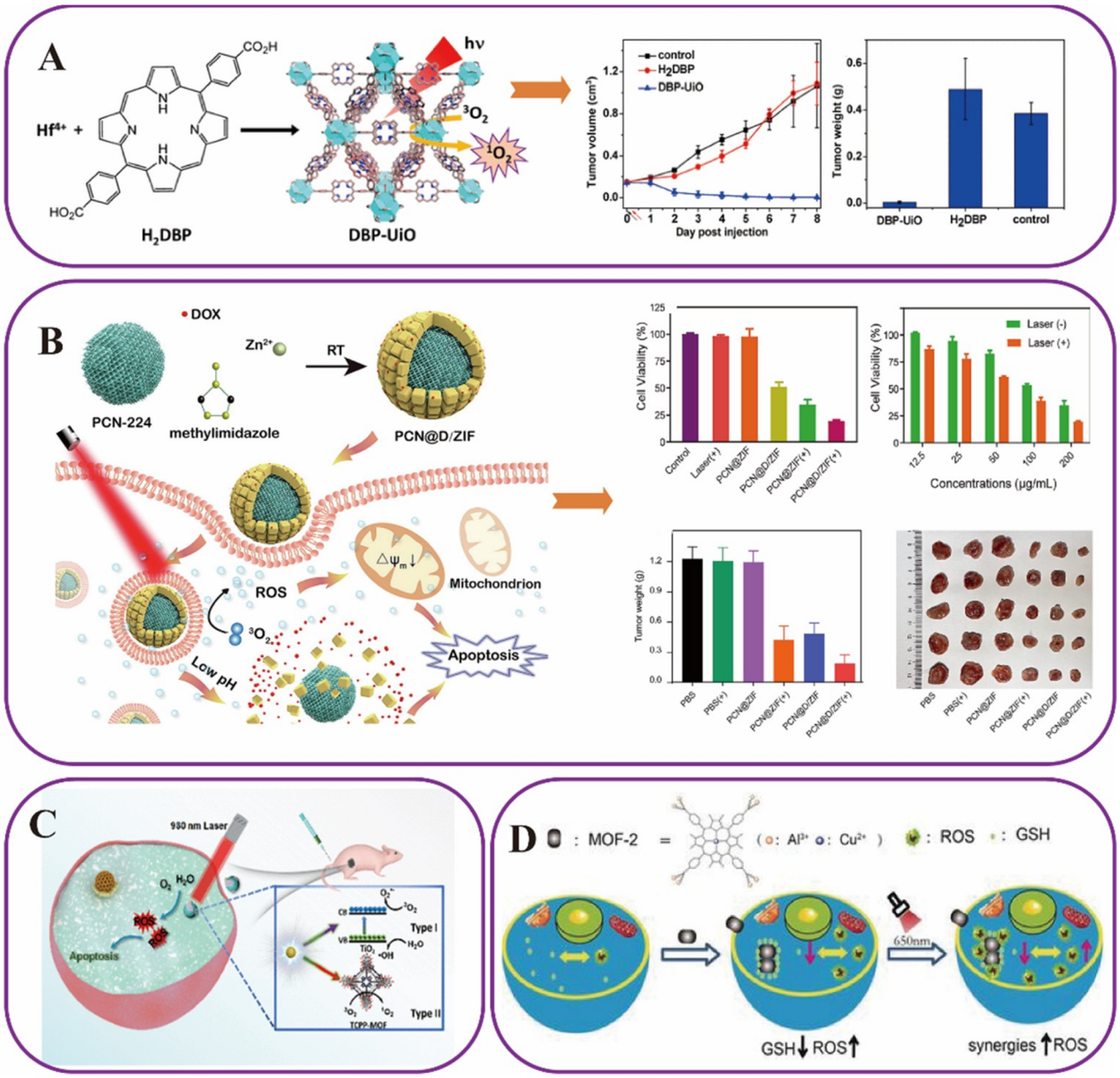

Fig. 3 (A) Synthesis process of DBP-Hf and the pathway of its PDT effect. The experimental results showed that DBP-Hf treatment had a significant reduction in tumor volume in half of the mice.[111] Panel (A) reproduced from ref. 111 with permission from American Chemical Society, copy 2014. (B) Schematic diagram of PCN@D/ZIF used in PDT/chemotherapy combination therapy. As shown, treatment of MCF-7 cancer cells with PCN@D/ZIF(+) produced 80.1% cytotoxicity, which was much higher than that produced by cells treated with PCN@D/ZIF(45.3%) or PCN@ZIF(+) (56.6%). When cells were treated with PCN@ZIF(+) or PCN@D/ZIF alone, the tumor inhibition rate was 47.9% and 38.9%, respectively. However, when cells were treated with PCN@D/ZIF(+), the best anti-tumor inhibition effect (66.5%) was obtained. The results showed that PCN@D/ZIF had good anti-tumor properties under light irradiation *in vivo* and *in vivo*.[116] Panel (B) reproduced from ref. 116 with permission from Elsevier, copy 2023. (C) The constructed UMOF-TiO_2 exerted both type I and type II PDT processes.[117] Panel (C) reproduced from ref. 117 with permission from American Chemical Society, copy 2020. (D) Schematic diagram of MOF-2 and mechanism of PDT. As shown in the figure, MOF-2 can efficiently adsorb glutathione (GSH), thereby reducing its level and increasing ROS production, and the photodynamic therapy effect is further enhanced after 650 nm laser irradiation.[118] Panel (D) reproduced from ref. 118 with permission from John Wiley and Sons, copy 2018.

of DBP-Hf, which greatly improves the light trapping efficiency. The coordination between DBC and Hf^{4+} resulted in an enhanced inter-system crossover (ISC), resulting in a 200-fold decrease in fluorescence intensity and more energy being used for $^1O_2$ generation rather than heat dissipation. Lin *et al.* provided a good idea for the application of MOFs in PDT and laid a good foundation for the follow-up. With the deepening of research, we found that the accurate role of materials in the tumor site is the key to our pursuit of precision cancer treatment. To date, no relevant nanomedicines have been successfully translated into clinical practice, mostly due to the poor targeting of the materials or the complex manufacturing

process. In order to improve the precise delivery of materials at the tumor site, Ma *et al.* demonstrated for the first time that H_2S-activated hybrid metal MOFs, $\{Cu_2(ZnTcpp)\cdot H_2O\}_n$ (designated NP-1), can be activated by hydrogen sulfide (H_2S) in the specific tumor microenvironment to effectively kill tumor cells[115]. NP-1 uses zinc metalized 5,10,15,20-tetra-(4-formate phenyl)porphyrin (ZnTcpp) as the ligand and copper (Cu^{2+}) as the node. The main mechanism of action of the material in the blood circulation, Cu^{2+} quenched the fluorescence of ZnTcpp through coordination and inhibited its photosensitive activity. When the material was in tumor cells, due to the rich hydrogen sulfide (H_2S) in the specific microenvironment of the tumor, Cu^{2+} reacts with H_2S and dissociates from the framework. To restore the luminescence and photosensitivity function of ZnTcpp. Structurally, Zn^{2+} occupies the porphyrin center, and NP-1 also has a two-dimensional (2D) layer network structure. These parallel layers interlock with each other and are further stacked into a 3D supramolecular structure through weak interactions. The 3D supramolecular structure provides 85.7% photosensitizer loading, far beyond the loading capacity of single metal MOFs. For therapeutic use, the activated ZnTcpp is irradiated with near-infrared light (600 nm) to transfer energy to the surrounding oxygen to efficiently generate highly oxidative $^1O_2$. Since H_2S is only enriched in the tumor microenvironment, NP-1 activation, and $^1O_2$ release are highly targeted, reducing damage to normal tissues. This study provides a novel H_2S-responsive photosensitizer platform for cancer precision therapy. The development of well-defined hybrid MOF for MOF-on-MOF growth has attracted much attention. Studies have shown that the MOF-on-MOF in hybrid MOFs can play a role in chemotherapy and photodynamic therapy. MOF-on-MOF in hybrid MOFs refers to the *in situ* growth of a second MOF with different composition or structure on the existing MOF crystal nucleus, forming hierarchical heterogeneous structures such as core–shell, hollow multi-shell, and core–satellite. This enables the realization of multiple properties that a single MOF cannot possess simultaneously. Liu *et al.* reported a zeolite imidazole ester skeleton (ZIF-8) that encapsulates DOX on the surface of Zr-based porphyrin MOFs[116] (Fig. 3B). PCN@D/ZIF not only can grow ZIF-8 without any modification of PCN-224, but also the layer thickness of ZIF-8 can be controlled. PCN@D/ZIF releases DOX from ZIF-degradation in the acidic environment of the tumor, and porphyrin MOF produces a large amount of singlet oxygen under light, which has a tumor-killing effect.

In 2019, Lin *et al.* reported the synthesis of a novel MOFs, Ti–TBP, and introduced its application in type I PDT.[119] The MOFs are synthesized by Ti-oxo chain SBUs and photosensitizing 5,10,15,20-tetra(*p*-benzoato)porphyrin (TBP) ligands, for hypoxia-tolerant type I PDT. It was found that Ti–TBP not only produces singlet oxygen under light, but also transfers electrons from the excited TBP to the SBUs of Ti^{4+} groups to generate superoxide, hydrogen peroxide, and hydroxyl radicals, resulting in ROS generation. At the same time, $TBP^{\bullet+}$ can also trigger oxidative stress by oxidizing glutathione (GSSG) to glutathione disulfide. The four different ROS-producing abilities enable Ti–TBP-mediated PDT to achieve a tumor regression rate of over 98% and a cure rate of 60%, which plays a huge role in the treatment of tumors. Since a single PDT mode (such as using only type II PDT) has limited efficacy in hypoxic tumors, while type I PDT can still function under hypoxic conditions, combining the two mechanisms can complement each other and improve the therapeutic effect.[120] It has been proposed that by combining type I and type II PDT, multi-mode synergistic treatment can be achieved to overcome the limitations of a single treatment mode.[121] In 2020, Dong *et al.* synthesized UCNP (lanthanide-doped upconversion nanoparticles) and meso-four(4-carboxyphenyl)methylene (TCPP)-MOF to form a heterodimeric UMOF, and further coated with ultra-small TiO_2 nanoparticles into UMOF-TiO_2 to achieve 980 nm near-infrared (NIR) laser-triggered type I and type II PDT[117] (Fig. 3C). Without further tedious chemical modification, the UMOF-TiO_2 nanocomposites exhibit high stability, excellent biocompatibility, and water dispersion due to the MOFS-based support and hydrothermal treatment. Through 980 nm laser rays, with deep biological tissue penetration and minimal photodamage, UCNPs were able to emit UV and visible light to stimulate TiO_2 and MOFs, respectively, effectively producing different kinds of highly cytotoxic ROS to induce apoptosis of cancer cells *in vitro* and *in vivo*. UMOF-TiO_2 showed significant tumor volume reduction and prolonged survival time in a mouse model without obvious systemic toxicity, indicating its promising application as a photodynamic agent. Because type I PDT shows hypoxia tolerance and type II PDT shows high responsiveness, scientists have creatively combined type I and type II PDT to achieve multimodal PDT treatment, which has far-reaching significance for the biomedical application of PDT. Moreover, subsequent research can also realize the combination of type I and type II PDT by developing novel photosensitizers (such as covalent organic framework COFs, organic small molecule photosensitizers, *etc.*) to improve the therapeutic effect.

It is well known that the generation efficiency and level of ROS play a very important role in PDT. Chen *et al.* constructed HA-DQ@MOF nanocarriers to achieve stable co-delivery of DTC and Cu^{2+} and effectively prevent their contact, thereby avoiding the premature formation of potentially toxic $Cu(DTC)_2$ complexes during *in vivo* circulation. This system utilizes the overexpressed ROS in the tumor microenvironment to trigger a dual activation mechanism: on one hand, it specifically cleaves HA-DQ to release DTC, immediately chelating Cu^{2+} to form highly active $Cu(DTC)_2$ to exert chemotherapy effects; on the other hand, it promotes the dissociation of MOF to release Zn-TCPP to restore the PDT activity. This cascading activation not only achieves a precise transformation from a low-toxic prodrug to a high-toxic treatment, but also significantly enhances the tumor-killing efficacy through the synergistic effect of $Cu(DTC)_2$ chemotherapy and Zn-TCPP PDT.[122] However, GSH, as an oxidant widely present in the human body, can reduce the concentration of intracellular ROS, especially cancer cells usually produce higher levels of GSH to adapt to high oxidative stress and protect themselves.[123] Therefore, it has become an urgent hope for scientists to synthesize a material that can produce ROS and reduce the level of GSH in cells. In 2018, Zhang *et al.* synthesized a MOF-2 based on Cu II as the

active center for PDT[118] (Fig. 3D). Experiments show that MOF-2 can produce a large amount of ROS when absorbed by tumor cells under light irradiation. At the same time, intracellular GSH was significantly reduced. This not only increased ROS concentration and accelerated cell apoptosis, thereby enhancing the effect of PDT (Fig. 3D). This experiment provides strong evidence for MOFs as promising new candidates for PDT and anti-cancer drugs. In 2021, Sun *et al.* decorated Cu-based MOFs HKUST-1 onto the surface of Ag NP to form Ag@HKU and further decorated with hyaluronic acid (HA) to construct a GSH-activated nanoplatform (Ag@HKU–HA).[124] GSH in the tumor microenvironment reduces Cu^{2+} to Cu^{+}, triggering HKUST-1 degradation, exposing Ag NPs, and promoting their oxidation to Ag^{+}. The obtained nano-delivery system not only avoids premature Ag leakage in the blood circulation, but also realizes the precise release of Ag at the tumor site. Moreover, Ag NPs were oxidized to toxic Ag^{+} in the tumor environment, and Ag^{+} induced cell death through mitochondrial damage and apoptosis. The generated Cu^{+} can catalyze endogenous H_2O_2 to highly toxic $^{\cdot}OH$ through a Fenton-like reaction, which opens up a broad idea for the use of PTT therapy and PDT therapy for synergistic treatment. Improving the hypoxic microenvironment can enhance the therapeutic effect of tumors and maximize the effect of the nano-drug delivery system. Chen *et al.* developed Ce6@HGMOF nanoparticles composed of a photosensitizer (Ce6), a glucose oxidase (GOX), a chemotherapeutic drug (HCPT), and an iron-based organic framework (MOF) to exert anti-tumor effects in a compound mode[125] (Fig. 4). In this nano-drug delivery system, GOX uses "starvation therapy" to consume glucose, starve the tumor cells, and produce gluconic acid and hydrogen peroxide. At the same time, Ce6@HGMOF can exert the catalytic activity of a nano-enzyme to generate oxygen, thereby improving the hypoxic microenvironment of the tumor. The improvement of the hypoxic environment in tumor tissue can help to slow down the growth of tumor blood vessels and improve the microenvironment of drug resistance to a certain extent. Moreover, it can enhance the therapeutic effect of PDT and enhance the oxidative stress response caused by ROS in tumors. In order to reduce the GSH of tumor cells, Ce6@HGMOF also plays an important role in it, and it can also induce ferroptosis of tumor cells through the Fenton reaction with H_2O_2. Ce6@HGMOF not only kills tumor cells at the level of PDT alone, but also plays a synergistic role in ferroptosis and starvation therapy. This innovative synergistic strategy not only plays a role in photodynamic therapy but also improves the tumor microenvironment and enhances the therapeutic effect of chemotherapy drugs and photodynamic therapy, which is a relatively new anti-tumor paradigm.

4.2 Application of MOFs in PTT

PTT therapy uses PTCA to absorb laser light of a certain wavelength, and rapidly convert the absorbed light energy into heat

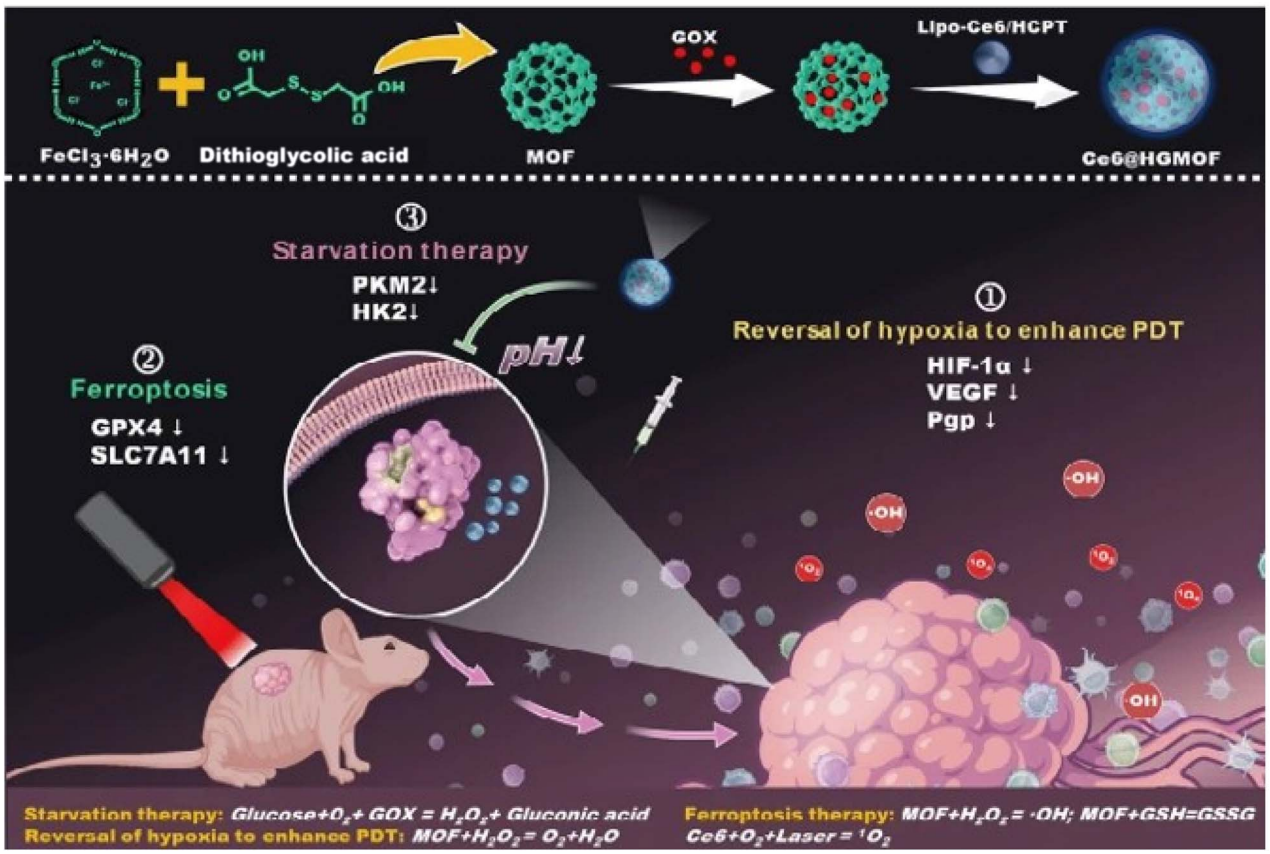

Fig. 4 The synthesis process and mechanism6 of Ce6@HGMOF,[125] reproduced from ref. 125 with permission from Springer Nature, copy 2024.

energy to kill cancer cells through the generated heat. Since PTT can be precisely targeted with the help of laser and can only irradiate the cancer area without affecting normal tissues, PTT has good selectivity and low invasiveness.[126]

MOFs play a very active role in PTT, generally in the following three ways: the first is that MOFs themselves play a photothermal conversion performance as PTCA for PTT treatment. Due to their structural diversity and design ability, MOFs materials can realize the absorption and conversion of light at different wavelengths by selecting different metal ions, organic ligands, or adjusting synthesis conditions. This characteristic makes MOFs can be used as an efficient PTCA to convert the absorbed light energy into heat energy, thereby killing cancer cells. The second is that PTCA is involved in the surface modification of MOFs. In order to improve the photothermal conversion efficiency of MOFs, scientists usually optimize their structure. For example, by introducing metal ions with high photothermal conversion efficiency (such as noble metals, combined polymer coatings, *etc.*), the photothermal performance of MOFs can be significantly improved. The third is the incorporation of PTCA into the porous structure of MOFs to exert PTT treatment. Moreover, MOFs can be retained in the target site for a long time, thereby improving the bioavailability of drugs. Next, we will specifically introduce the application of MOFs in PTT therapy according to the above three methods.

Porphyrins are macromolecular heterocyclic compounds composed of porphyrin ($C_{20}H_{14}N_4$).[127] Porphyrins and porphyrin derivatives have excellent photophysical and electrochemical properties. In biomedical applications, they have effective biological properties, such as biocompatibility, effective clearance, longer residence time in tumors, fewer side effects, and imitation of various biological functions. However, they have some disadvantages, such as instability under physiological conditions, easy self-quenching, *etc.*[128] The application of porphyrins in phototherapy is limited. To overcome these problems, porphyrin-based MOFs have been developed by introducing porphyrin molecules into MOFs or using porphyrin as an organic linker, based on the fact that MOFs are composed of metal ions/SBUs and organic connectors.[129,130] Porphyrin-based MOFs overcome the limitations of porphyrins.[131] In 2018, Zhang and his team synthesized a novel zirconia–iron–porphyrin MOFs (Zr–FeP MOFs) nanoparticle using a simple one-pot method[132] (Fig. 5A–C). Experiments show that under near-infrared (NIR) laser irradiation, Zr–FeP MOFs nanoparticles not only can produce a large number of ROS, but also exhibit significant photothermal effects, with a photothermal conversion rate as high as 33.7%. Moreover, siRNA/Zr–FeP MOFs loaded with heat shock protein 70 siRNA significantly inhibited tumor growth both *in vivo* and *in vitro*. In terms of imaging, it also has the characteristics of photothermal imaging, CT imaging, and photoacoustic imaging, which can be applied to tumor diagnosis. siRNA/Zr–FeP MOFs integrate photothermal, photodynamic and imaging diagnosis, which shows the broad prospects of nanomaterials in biomedical applications. NIR photothermal materials convert the absorbed NIR light into thermal energy by inhibiting the radiative transition.[133] Perylene imides are fluorescent dyes with excellent

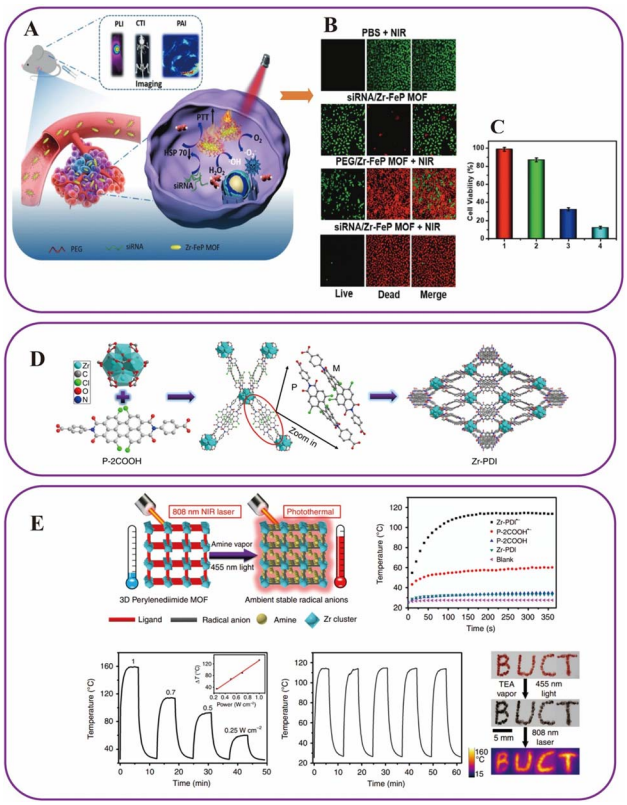

Fig. 5 (A) Diagnostic and therapeutic process diagram of siRNA/Zr–FeP MOF. (B and C) Schematic representation of cell viability and confocal laser scanning microscopy images after different treatments. The results showed that the siRNA/Zr–FeP MOF treatment group had the most efficient anti-tumor ability, with a cell death rate as high as 87.5%. The Zr–FeP MOF showed a good anti-tumor ability even after laser irradiation. The introduction of siRNA effectively inhibited the expression of Hsp70, which is considered to be a key factor in thermal resistance, and further increased the anti-tumor effect.[132] Panel (A–C) reproduced from ref. 132 with permission from John Wiley and Sons, copy 2018. (D) Synthesis process of Zr–PDI. (E) Related experiments demonstrated good photothermal properties of Zr–PDI. As shown in the figure, the photothermal conversion efficiency and photothermal stability of Zr–PDI are superior.[134] Reproduced under a Creative Commons CC BY Attribution 4.0 International License.[134]

light, thermal and chemical stability, and their anion free radicals have strong near-infrared absorption characteristics. However, the anion free radicals are easily oxidized in the air and affect their use. So it is of great significance to find a way to stabilize anion-free radicals in the air. In 2019, Yin *et al.* used carboxylic acid–perylene imide (P–2COOH) to form 3D MOF (Zr–PDI) by solvothermal reaction with $ZrCl_4$ in dimethylformamide. Zr–PDI is the first 3D perylene imide (PDI) MOF, which not only shows high stability and high porosity, but also the 3D porous network formed by Zr–PDI can be used as a cage to trap electron donors, such as organic amines, it provides an extremely stable anion radical ($Zr\text{–}PDI^{\bullet-}$) *in situ* through photoinduced electron transfer (PET), while $Zr\text{–}PDI^{\bullet-}$ has a strong near-infrared absorption characteristic and can rapidly heat up under 808 nm near-infrared laser irradiation[134] (Fig. 5D and E). Under 808 nm laser irradiation, the temperature

of Zr–PDI$^{\bullet-}$ powder reached 160 °C within 10 seconds, and the temperature of Zr–PDI$^{\bullet-}$ film immobilized on quartz glass rose over 89 °C within 200 seconds, showing an extremely high photothermal conversion efficiency (52.3%). This indicates that Zr–PDI$^{\bullet-}$ powder is a material with excellent photothermal conversion efficiency and stability, which is expected to become a promising therapeutic agent in photothermal therapy if it can be realized for biomedical applications. In 2020, Deng *et al.* developed ultra-thin (16.4 nm thick) ferrocene-based MOF (Zr–Fc MOF) nanosheets for synergistic PTT and Fenton reaction-based chemokinetic (CDT) therapy to cure cancer without additional drugs[135] (Fig. 6). The Zr–Fc MOF nanosheets not only exhibited a good photothermal conversion efficiency (53%) but also acted as an effective Fenton catalyst to promote the conversion of H_2O_2 to hydroxyl ($^{\bullet}OH$). This multi-therapeutic approach to synthesize a therapeutic platform for MOFs may open a new era in the research of MOF-based collaborative therapeutic platforms for cancer.

Nowadays, many metallic materials, such as Au, Ag, and Pt, have been used in PTT research. Due to its easy surface modification and unique optical and electronic properties, gold nanomaterials have been widely used in the regulation of photothermal effects.[136] Therefore, scientists often modify Au NPS into various structures or combine them with other structures, expecting to achieve a more effective effect. In 2017, Zeng *et al.* constructed a core–shell gold nanorod@MOFs (AuNR@MOFs). The scientists chose AuNR as seed crystals, and then Zr-based porphyrin MOFs were grown on the AuNR surface, and finally loaded with chemotherapy drug camptothecin (CPT) to achieve cancer treatment[137] (Fig. 7A–C). AuNR@MOFs@CPT, as a multifunctional therapeutic nanoplatform for tumor photodynamic/thermal/chemical combined therapy, has shown excellent tumor treatment ability. The results showed that the photothermal conversion efficiency of the unloaded AuNR@MOFs solution was 20.6% by 808 nm laser irradiation *in vitro*, and the CPT loading still maintained strong photothermal responsiveness. Under the laser illumination of 660 nm, the MOFs shell produced a large number of ROS, and a large amount of singlet oxygen ($^1O_2$) was detected. In addition, 808 nm laser irradiation accelerates the release of CPT from the MOFs pore. *In vivo*, dual light irradiation (660 nm PDT + 808 nm PTT) showed a tumor inhibition rate of 83% and a more than 90% reduction in tumor volume compared with the control group, without significant toxicity. AuNR@MOFs@CPT showed significant anticancer properties both *in vivo* and *in vitro*. Not coincidentally, in 2024, Nejad *et al.* decorated Au-NPs on the surface of MOFs (PCN-22) by a one-pot method. The experimental detection found that PCN-224/Au-NPs showed significant anticancer activity against tumor cells and good biocompatibility with normal cells, and the synthesis method of this method is simpler and greener.[138] In order to reduce the adverse reactions of patients, monoclonal antibodies (mAbs), peptides, oligosaccharides, small molecules, and aptamers are often linked to nanomaterials to improve the targeting of drugs.[139] In 2021, Chien *et al.* synthesized MCP-1/GNR@MIL-100(Fe).[140] Since CTAB on the surface of gold nanorod is highly cytotoxic, 11-mercaptoundecanoic acid (MUA) was used to form a self-assembled monolayer to reduce the toxicity of the material. To enhance the biocompatibility of the material, MIL-100(Fe) was coated on the outside of the gold nanorod. To enhance the targeting property of the material, we coated MIL-100(Fe) on the surface of the nanorods with MCP-1 peptide, and then used the tumor homing ability of macrophages to achieve active targeting to accumulate the material at the tumor site. Finally, GNR was induced by NIR 808 nm laser irradiation to kill tumor cells. The results showed that the loading of MCP-1 reached 5.52%, and the migration rate of macrophages was increased after modification, and the endocytosis of the material by macrophages was increased, which greatly strengthened the targeting ability of the material. To solve the problem of uneven distribution of traditional nanocarriers by penetrating the hypoxic region of the tumor mediated by macrophages. In

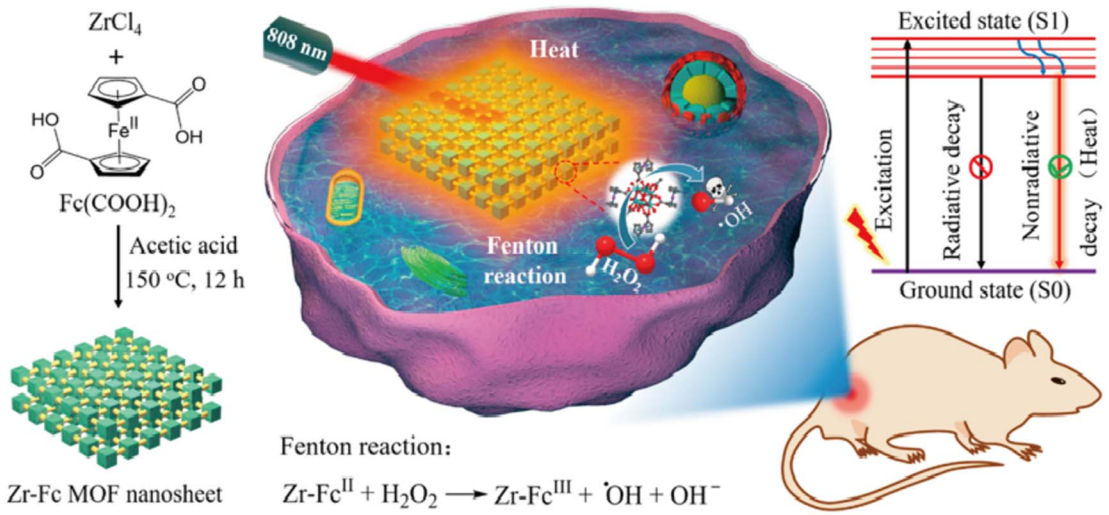

Fig. 6 Schematic diagram of the synthesis of Zr–Fc MOF and its photothermal effect, reproduced from ref. 135 with permission from American Chemical Society, copy 2020.

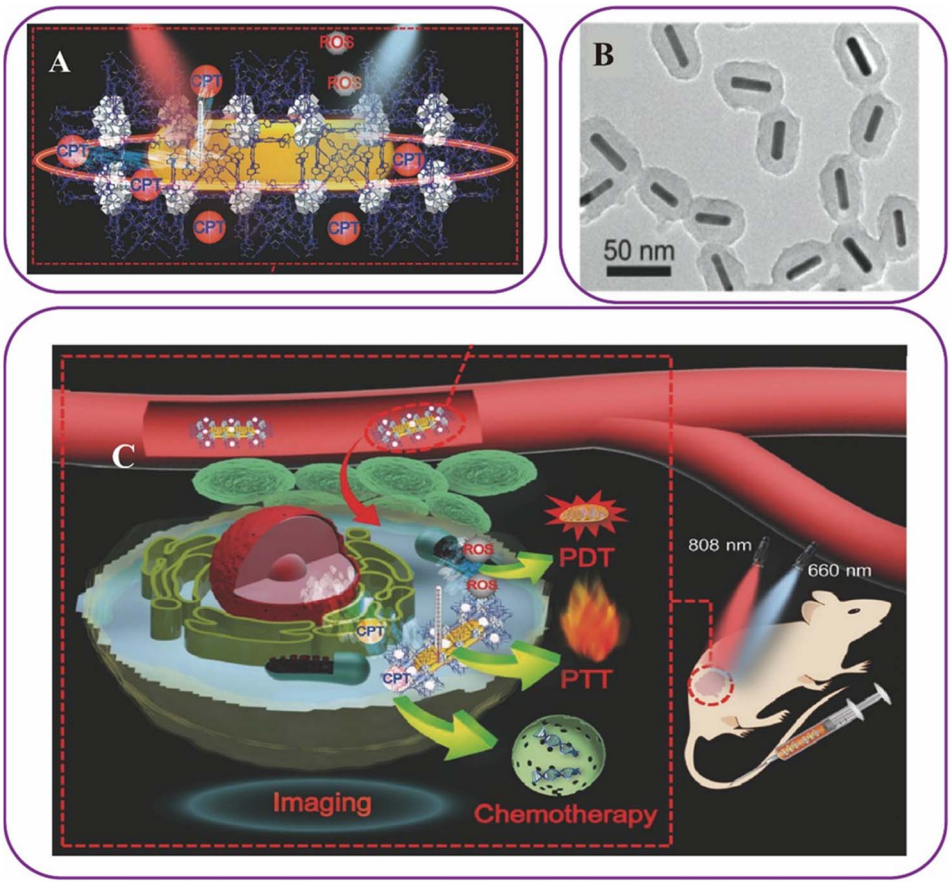

Fig. 7 (A) Structural diagram and mechanism of action of AuNR@MOFs@CPT. (B) AuNR@MOFs schematic diagram of transmission electron microscopy. (C) How AuNR@MOFs@CPT acts *in vivo*.[137] Panel (A–C) reproduced from ref. 137 with permission from John Wiley and Sons, copy 2017.

this experiment, macrophages can penetrate the vascular barrier to reach the hypoxic region of tumors, and the constructed nanodrug delivery system has stronger targeting and uptake ability, which enables the gold nanorods to play a stronger photothermal effect, all of which provide more perspectives for the design of multifunctional nanomaterials for biomedical applications.

In addition, it is also one of the common strategies to exhibit a strong absorption coefficient and excellent photostability by combining polymer coatings such as polyaniline (PAN) compared to the widely used inorganic gold, carbon-based near-infrared photothermal agents (PTA), and organic dyes. In 2016, Jing *et al.* constructed hybrids, namely UiO-66@PAN, from nanoscale MOFs UiO-66 and nano-absorbable polymers (PAN).[141] Experiments showed that mice injected with UiO-66@PAN maintained local tumor temperature at 42 to 45 °C for 10 minutes under laser irradiation (808 nm, 0.7 W cm^{-2}) during 10 days of treatment. Notably, the ablated tumors turned into black scars *in situ*. After 10 days of treatment, tumors completely regressed in mice treated with UiO-66@PAN and NIR irradiation, while tumors in the control or UiO-66@PAN only groups were significantly larger in size. The calculated tumor suppression efficiency was about 93%. Experiments have shown that UiO-66@PAN has suitable size, good water dispersion, strong near-infrared absorption, high photostability and photothermal conversion efficiency. Moreover, UiO-66@PAN is effective for PTT-based cancer therapy *in vitro* and *in vivo*. In 2017, Xie *et al.* synthesized UIO-66@CYP with bioimaging and PTT activity by polymerizing a NIR dye cyanine-containing polymer (CyP) *via* Passerini reaction on the basis of a Zr-based MOFs (UiO-66)[142] (Fig. 8A). *In vitro* and *in vivo* experiments have proved that UiO-66@CyP is very effective for PTT-based cancer therapy. The synthesis of polymer-MOF hybrids opens up prospects for the production of a variety of similarly structured nanostructures.

The new indocyanine green (IR-820) has similar properties and structure to indocyanine green (ICG). Compared with ICG, IR-820 is more stable and has good biocompatibility. As nanomaterials with a high specific surface area, MOFs can encapsulate the photosensitizer molecules in the framework, which can effectively reduce the self-aggregation and self-quenching of common photosensitizers, and improve their water solubility to maximize the utilization of photosensitizers. In 2024, Huang *et al.* loaded DOX and IR-820 onto MIL-101(Fe) by a physical adsorption method with a polymeric dopamine coating on the surface to prevent drug leakage.[144] The PDA is covalently linked

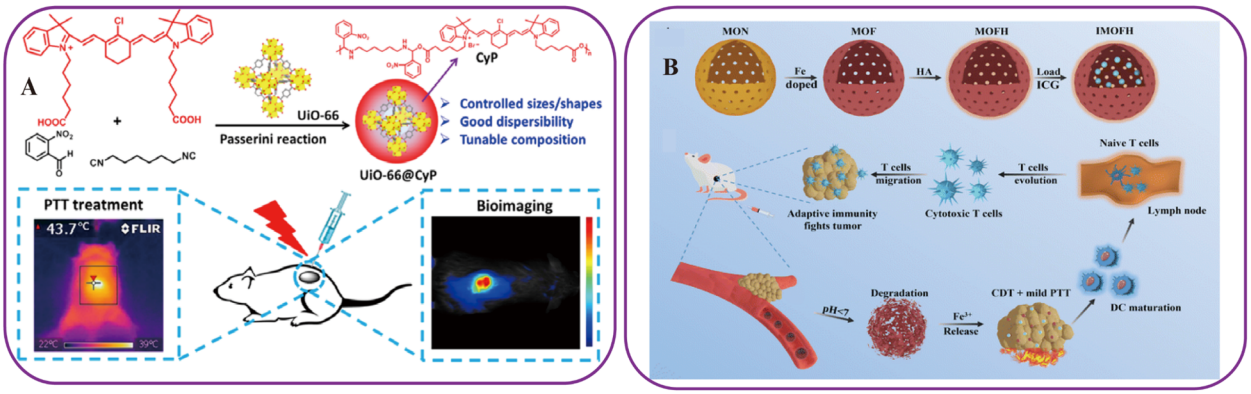

Fig. 8 (A) Synthesis process and mechanism of action of UiO-66@CyP.[142] Panel (A) reproduced from ref. 142 with permission from American Chemical Society, copy 2017. (B) Schematic of the preparation of IMOFH and the synergistic effect of the anti-tumor ability of IMOFH in combination with mild PTT.[143] Panel (B) reproduced from ref. 143 with permission from Royal Society of Chemistry, copy 2022.

to the $-NH_2$ group provided by the synthetic polymer NH_2–PEG–OCH_3/F3 for targeted drug delivery. ID@MIL-PPF3 had a good drug loading rate (27.7%) and photothermal conversion efficiency (28.89%). Studies have shown that ID@MIL-PPF3 can produce a large amount of ROS and heat after laser irradiation, achieve the synergistic effect of photothermal/photodynamic/chemical dynamic therapy, and has good tumor targeting and stability, which is a potential cancer therapeutic agent. In the research on tumor therapy, T cells are inevitably mentioned. Studies have shown that T cells can kill tumor cells, but they have the disadvantages of immunosuppression and a lack of targeting. Nowadays, the use of immunotherapy to treat cancer is becoming more and more possible. Due to the immune escape mechanism of cancer cells, the application of immunotherapy can play a strong role in anti-tumor cells. MOFs can be used as a delivery system to deliver proteins and other substances in immunotherapy. Or they can be used as a part of immunotherapy.[145] Lan *et al.* reported a metal–organic framework material named Fe–TBP as a new type of nano-light sensitizer. It can overcome the hypoxic condition of tumors and make photodynamic therapy effective, thereby initiating cancer immunotherapy for non-inflammatory tumors.[146] Yang *et al.* first prepared mesoporous organosilicon dioxide nanoparticles (MON) and then Fe^{3+} loaded MON (MOF), and finally modified with HA and loaded with ICG to obtain IMOFH[143] (Fig. 8B). In the acidic environment of tumors, Fe^{3+} is released and mediates oxidative cell death, which cooperates with ICG's mild PTT effect to facilitate the release of tumor-related antigens, thereby enhancing immunogenicity. *In vivo* experiments further showed that mild PTT promoted IMOFH-mediated DC maturation and $CD8^+$ T cell infiltration. This is an innovative immunotherapy approach for TNBC tumors that combines the catalytic oxidation damage of tumor cells by nano-drugs with mild photothermal therapy, laying a solid foundation for the combination of various treatment methods using MOFs in the future.

4.3 Synergistic therapy of PDT and PTT mediated by MOFs

Nowadays, the focus of cancer treatment has shifted from cytotoxic non-specific chemotherapy to molecular targeted and rationally designed therapies, which have shown higher efficacy and fewer side effects.[147] Traditional chemotherapy has the disadvantages of lack of targeting ability, systemic toxicity and side effects. Moreover, most anticancer drugs are poorly soluble in water. With the continuous progress of research, scientists are no longer satisfied with a single treatment method, they combine various treatment methods, hoping to play a greater role in anti-tumor effect, and can reduce the side effects. The construction of nano-targeted drug delivery system can not only target high-dose chemotherapy to the target area, but also preserve healthy tissues, overcoming the limitations of traditional chemotherapy.

PDT and PTT therapies are limited by the complexity and hypoxia surrounding the tumor tissue in practical applications. In order to overcome the limitation of hypoxia, Liang *et al.* prepared nanoparticles FI@FM5 composed of ICG and Fe-MOF-5, which showed good optical effects.[148] Experiments show that Fe-MOF-5 not only has the best nano-enzyme activity, which can promote the decomposition of hydrogen peroxide and improve the hypoxic environment of tumors, but also has excellent photothermal conversion efficiency, which can produce ROS under the irradiation of 808 nm laser to play a role in PDT. The improvement of tumor hypoxia environment can increase the therapeutic effect of PDT and PTT, forming a virtuous circle. It provides new ideas for the application of MOFs as important carrier materials in the field of phototherapy by constructing a relatively stable nano-targeted drug delivery system and actively seeking to improve the tumor hypoxic microenvironment. Lin *et al.* added the function of targeted fluorescence imaging on the basis of regulating tumor hypoxic microenvironment[149] (Fig. 9). ICG–PFH/MOF/DNA–Dox has the MOF as the core, loaded with ICG and perfluorohexane (PFH), and finally double-stranded nucleic acid (dsDNA) as the shell, which encodes ATP aptamer and AS1411 aptamer and is anchored by doxorubicin (Dox). ICG–PFH/MOF/DNA–Dox can not only

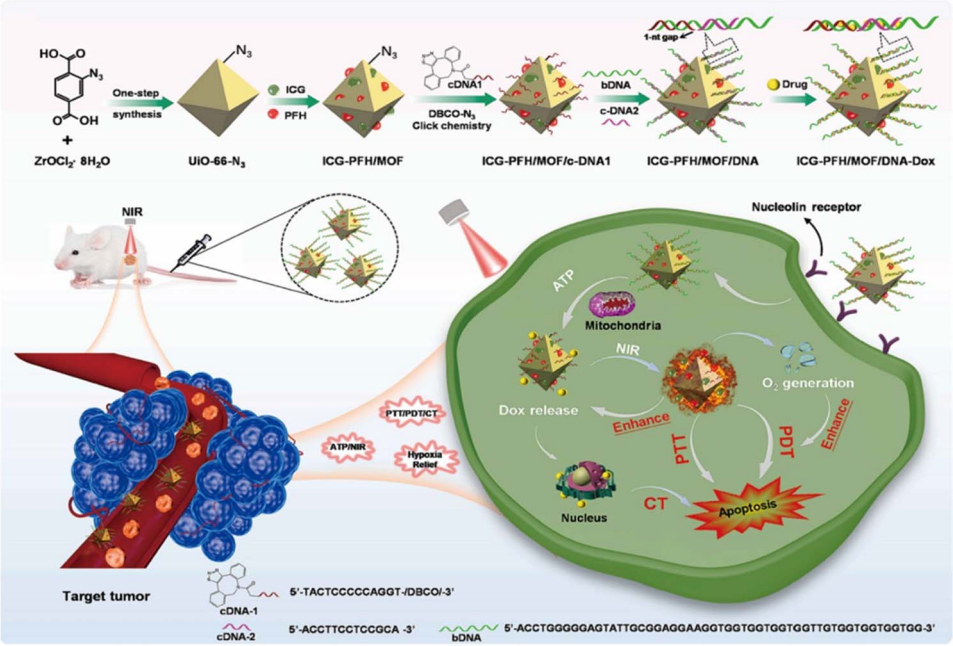

Fig. 9 Schematic diagram of ICG–PFH/MOF/DNA–Dox preparation and the mechanism of combined therapy, reproduced from ref. 149 with permission from Elsevier, copy 2024.

identify tumor cells to actively target and release Dox for chemotherapy, but also exert PTT and PDT effects under laser irradiation. In particular, the loaded PFH can be used as an O_2 supply agent to alleviate the hypoxic environment of tumors. This therapeutic platform that not only relives the hypoxic environment, but also combines the therapeutic effect of tumor treatment is surprising and worthy of subsequent reference. Due to its effectiveness in promoting various catalytic reactions, Wang *et al.* shifted their attention to single-atom catalysts (SACs) by synthesizing a MOF P-MOF rich in porphyrin-like monatomic Fe(III) centers.[150] Based on the abundance of single-atom Fe(III) centers, P-MOF materials showed excellent performance in regulating the hypoxic tumor microenvironment of mouse HeLa cell tumors, while also demonstrating their good performance as photoacoustic imaging (PAI) reagents; the narrow band gap energy (1.31 eV) of P-MOF can strongly absorb NIR photons, thereby causing a non-radiative transition, thereby converting the incident light into heat and playing a role in tumor PTT. In addition, under NIR irradiation, a slight change in the central spin state of monatomic Fe(III) in P-MOF converts coordinated triplet oxygen ($^3O_2$) to singlet oxygen ($^1O_2$), thereby benefiting PDT. The experimental results show that P-MOF plays a good role in PDT, PTT and tumor photoacoustic imaging (PAI), and the experiment also proves that single catalyst has great potential as a therapeutic platform for the construction of MOFs.

Since drug therapy is hampered by adverse off-target effects and uncontrolled release of therapeutic drugs, many efforts have been made to ameliorate this problem. In 2021, Cai *et al.* synthesized a nano-targeted drug delivery system Au@MOF-FA by using gold nanorods as the core, growing MOFs shells on the outer side, and finally surface modified with folic acid[151] (Fig. 10A and B). It is well known that Au can exert PTT effect, and the porphyrin ligand in the MOF shell can produce ROS under light conditions, thereby exerting PDT effect. Not only that, the metal node $Fe_3O(OAc)_6(H_2O)_3^+$ cluster of the MOF can decompose H_2O_2 and produce oxygen to improve the hypoxic environment of tumors and enhance the dual effect of PDT/PTT treatment. In addition, the folic acid modified on Au@MOF surface can make the nano-drug delivery system accumulate at the tumor site and increase the drug targeting. In 2022, Liu *et al.* first used 2-methylimidazole and zinc nitrate to generate MOFs material ZIF-8, then reacted with 2-methylimidazole, zinc nitrate and DOX to generate DOX/Z nanomaterials, and then adsorbed photothermal material ICG by electrostatic adsorption on the surface. Finally, FA–PEG was modified on the surface of DOX/Z-ICG by coordination to form DOX/Z-ICG–FA targeted nanodrug delivery system. In the synthesized DOX/Z-ICG–FA, ZIF-88 will degrade in the acidic condition of the tumor, releasing DOX to play the role of chemotherapy, ICG plays the photothermal properties, and FA plays the targeting property. The nano-systems can be taken up by tumor cells through the endocytosis mediated by FA receptors, thereby reducing the toxic side effects of the drugs.[152] In 2024, GAO *et al.* loaded the near-infrared dye IR-780 and the chemotherapy drug Dox together onto the MOFs material ZIF-8. Due to the bone marrow homing and homotypic targeting properties of the cell membrane of multiple myeloma, the cell membrane of multiple myeloma was encapsulated on the surface, forming a nano-targeted delivery system D/INPs@CM[153] (Fig. 10C). By examining the cellular uptake behavior of RAW264.7 and multiple myeloma cells against D/INPs@CM, the authors demonstrated

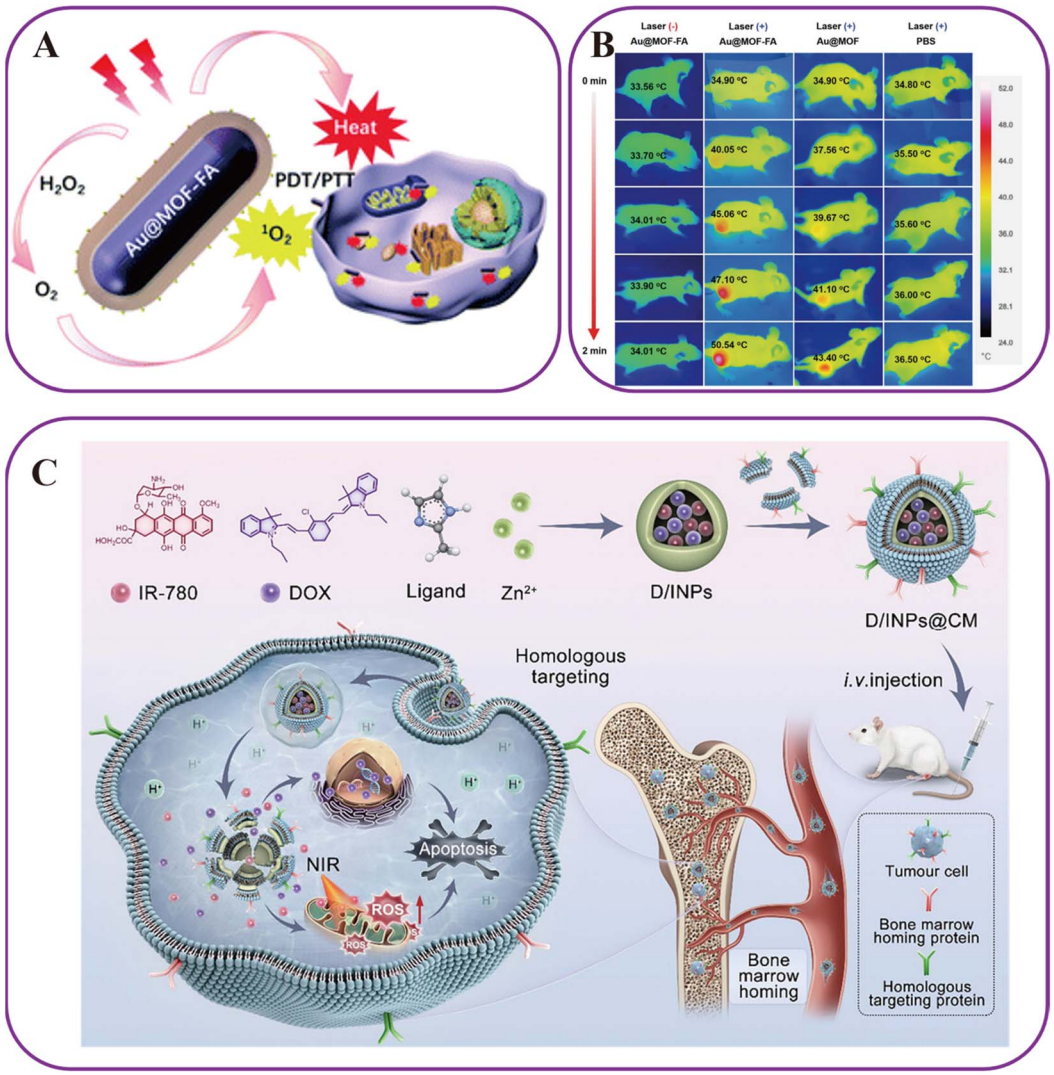

Fig. 10 (A) Au@MOF-FA Schematic diagram of the combined effect. (B) Schematic diagram of the temperature of the tumor site after illumination after different grouping, as shown in the figure, FA plays an excellent targeting role, so that Au@MOF-FA accumulates in the tumor site.[151] Panel (A) and (B) reproduced from ref. 151 with permission from Royal Society of Chemistry, copy 2021. (C) Preparation process and specific application mechanism of D/INPs@CM.[153] Reproduced under a Creative Commons CC BY Attribution 3.0 International License.[153]

that the system had immune escape ability, reduced macrophage phagocytosis, prolonged circulation time and homologous targeting ability. By loading two drugs, IR-780 and Dox, the system not only exerted the effect of chemotherapy, but also played the role of PDT and PTT. In the authors' experiments, the ROS level irradiated by NIR light was higher and the proportion of dead cells in the staining of live and dead cells was greater. *In vivo* experiments, the authors intravenously injected D/INPs@CM and D/INPs into mouse controls to demonstrate the targeting of multiple myeloma cell membranes to tumor sites. The above practice exploits the characteristics of high porosity, large surface area, and good biocompatibility of MOFs, making them ideal carrier for targeted drug delivery. Secondly, more efficient tumor-killing ability is achieved by introducing the synergistic effect of PTT, PDT and chemotherapy. Finally, targeted modification (such as folic acid modification) and biosimulation can improve the targeting of drugs and reduce side effects. The constructed nano-targeted drug delivery system can change the basic characteristics and biological activity of drugs, stay in the blood circulation for a longer time, and ensure the controlled release of drugs at a specified space and time. Compared with 1–10 μm particles, nano-scale materials can be integrated into the tissue system to promote cellular drug uptake, achieve effective targeted drug delivery, and ensure that the drug is effective at the target site.[154,155] The innovation of materials is also a great effort for MOFs in tumor therapy. Deng *et al.* focused their attention on a unique porphyrin derivative, formaldehyde, which has been proven to have extraordinary potential for phototherapy applications. Deng was the first to report the unique phosphorus corrole-based MOFs, Cor(P)–Hf, with a (3,18)-connected general topology, which is constructed by Cs-symmetric dicarboxylic acid ester 3 linkers, 10-fluorophenyl-5,15-diphenylphosphoric acid corrosive agent (Cor(P)) and a peculiar D_{3h}-symmetric 18-connected Hf_{12}-oxo

cluster, and possesses stability.[156] Not only that, they also mixed Cor(Fe) or Cor(Cu) as secondary functional connectors based on the mixed coro ligand MOFs Cor(P)/Cor(Cu)–Hf and Cor(P)/Cor(Fe)–Hf were constructed by simple "one-pot" solvothermal method, respectively. Furthermore, experiments show that Cor(P)/Cor(Fe)–Hf can play a good synergistic treatment method of PDT, PTT and CDT under laser irradiation in both *in vivo* and *in vitro* experiments. Such a simpler and more extendable experimental method and the innovation of experimental materials with good properties in phototherapy will continue to contribute to the establishment of anti-cancer nano platforms for MOFs.

Nowadays, the nano-targeted drug delivery system built by scientists no longer only meets the diagnosis or treatment of diseases, but combines the purpose of diagnosis and treatment to form a more promising system platform. In 2017, Liu *et al.* synthesized template NMOPs containing Mn^{2+} and IR825 and then mixed them with Hf^{4+} to obtain core–shell and codoped Mn/HF-IR825 NMOPs.[157] In the nano-targeted drug delivery system, each substance has its own function. For example, Mn^{2+}, high Z element Hf^{4+} and ligand IR825 are used as MRI contrast agents, CT signal enhancement and radiation sensitivity enhancement, and photothermal agent, respectively, to play a role in tumor diagnosis and treatment. The MOFs composite materials with imaging function created by the authors not only provide high MRI active substances for imaging purposes, but also provide the porosity of MOFs, which provides a good storage capacity for the delivery of therapeutic drug molecules, so that the diagnosis and treatment of diseases are combined, and it opens up a good prospect for the subsequent biomedical development. It is worth noting that the ability of MOFs to receive near-infrared (NIR) light absorption is also very important when used as drugs. Li *et al.* synthesized ultra-thin Cu-4(4-carboxyphenyl)porphyrin (Cu-TCPP) MOF nanosheets by a simple solvothermal method.[158] The experiments show that the ultra-thin Cu-TCPP MOF nanosheets not only have a strong NIR absorption ability, but also have good photothermal properties and can produce singlet oxygen, which plays an efficient role in the realization of PDT and PTT combined therapy. Moreover, ultra-thin Cu-TCPP MOF nanosheets also have excellent performance in titanium-weighted magnetic resonance (MR) imaging due to the unpaired 3d electrons of copper. Li *et al.* constructed promising nanoplatforms that combine phototherapy with imaging to realize a novel synthetic pathway for nanodrug delivery systems. In parallel, Cheng *et al.* proposed an all-in-one nano-targeted drug delivery system with tri-modality imaging-guided synergistic PTT/PDT/CDT[159] (Fig. 11A–E). In Cheng *et al.*, heating on the basis of a mixed metallic Cu/Zn-MOF resulted in a hollow porous structure with coexisting $Cu^{+/2+}$ to achieve ICG loading, and the subsequent heating treatment was used to integrate Mn^{2+} and MnO_2 in the presence of manganese(II) acetylacetonate. Under the irradiation of laser, ICG can not only display photothermal imaging and fluorescence imaging, but also play the role of PTT and PDT. Mn^{2+}/Cu^{+} react with H_2O_2 in a pseudo-Fenton-like reaction, generating cytotoxic $^{\cdot}OH$ to enhance CDT, while the decomposed oxygen can improve the oxygen demand of ICG-mediated PDT. Cu^{2+}/MnO_2 scavenges glutathione to improve ROS based therapies, while the Mn^{2+} formed are able to "turn on" magnetic resonance imaging. The biosafety profile of ICG is known to be excellent. This drug-free synergistic antitumor strategy not only achieves high therapeutic efficacy in normal tissues but also achieves low side effects for patients receiving the drug. Therefore, this multi-metal MOF plays an active role in the subsequent construction of a nano-drug delivery system platform with a combination of multiple methods, which not only improves the efficacy of tumor therapy, but also reduces the side effects of patient treatment and increases the happiness of patients.

Scientists often combine PTT, PDT, and chemotherapy, which can enhance the therapeutic effect of tumors through the complementation of multiple mechanisms. With the progress of nanomedicine and precision medicine, more and more combined targeted nano-drug delivery systems have appeared in front of patients. This multimodal strategy is expected to become an innovative treatment scheme for tumors, which opens up a very broad prospect for the diagnosis and treatment of tumor diseases.

5. Combining the MOFs response mode with PDT and PTT

The targeted nanodrug delivery system can release the encapsulated drug when it receives a certain stimulus, which can induce drug release at the expected site in a controlled manner, providing a good idea for the development of new drug preparations. Carrier MOFs can respond to any change in environmental conditions or signals by inducing changes in their chemical composition or physical structure to form a triggered response moiety.[160] The stimuli received by trigger-responsive MOFs can generally be divided into two broad categories: internal stimuli and external stimuli.[161,162] Internal stimuli depend on various physicochemical properties of the trigger site, including changes in intercellular pH, temperature, oxygen content, and REDOX potential.[163] The external stimuli (magnetic field, electric current, light and heat) are used to achieve the control and accurate regulation of drug release in the nanodrug delivery system (Fig. 12). One of the most widely used types MOFs in cancer treatment research is pH-responsive MOFs.[164] Due to the high proliferation and glycolytic stimulation of cancer cells, the pH value of the tumor microenvironment (TME) is acidic, and the intracellular changes are more significant. It is well known that the construction of dual-drug loaded nano-targeted delivery system is a complicated matter. Wu *et al.* cleverly took advantage of the feature that MOFs can be covalently linked with drugs, and prepared CMMOP by using Cu(II) and drug "Sawtooth" antibacterial inhibitor A4 (CA4) and mitoxantrone (MIT) as precursors.[165] Cu(II) was used as a bridge to connect and coordinate with the dual drug, and the total drug load of the constructed nano-targeted delivery system could reach 89%. At the same time, the coordination between Cu(II) and drug is very stable under normal physiological pH. At pH 7.4, 37 °C, CMMOPs only released 6.4% of CA4 and 10.2% of

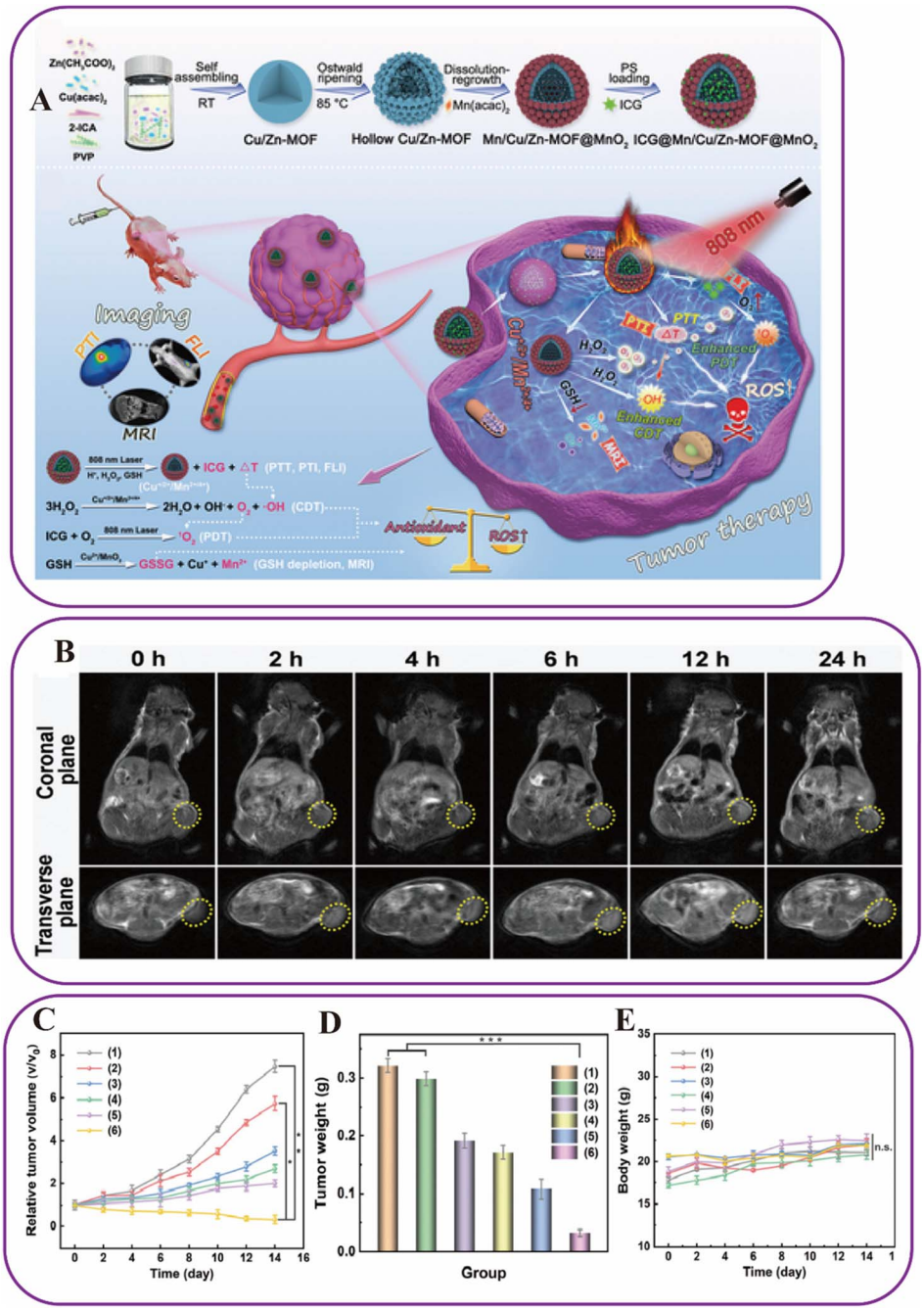

Fig. 11 (A) Schematic diagram of ICG@Mn/Cu/Zn-MOF@MnO_2 synthesis and its mechanism for combined diagnosis and treatment. (B) *In vivo* magnetic resonance imaging images of tumor bearing mice after intravenous injection of ICG@Mn/Cu/Zn-MOF@MnO_2. (C) Tumor growth curves after treatment in different groups. (D) Mean tumor weight after treatment in different groups. (E) Changes in body weight of mice. The mice were divided into: (1) normal saline group, (2) single laser group, (3) ICG + laser group, (4) hollow Cu/Zn-MOF group, (5) Mn/Cu/Zn-MOF@MnO_2 group, (6) ICG@Mn/Cu/Zn-MOF@MnO_2 + laser group. As shown in figure (B), ICG@Mn/Cu/Zn-MOF@MnO_2 showed good disease diagnosis ability. As shown in (C–E), ICG@Mn/Cu/Zn-MOF@MnO_2 has high tumor killing ability.[159] Panel (A–E) reproduced from ref. 159 with permission from John Wiley and Sons, copy 2021.

MIT for 48 h, but at pH 5.0, the cumulative release percentage of CA4 and MIT increased to 90.2% and 93.2%, respectively, and the burst release of both drugs was very sharp. This demonstrated the advantage of its easy cleavage in the acidic tumor microenvironment. The results show that CMMOPs exhibit excellent anti-tumor effects *in vitro* and *in vivo*, with high drug loading and pH responsiveness, and have great prospects in the targeted therapy of tumors. Similar to the pH response, the scientists transferred the stimulation conditions to ions in the human body. Ion-responsive MOFs are able to undergo structural or chemical changes when stimulated by specific ions, such as phosphate ions. Wang *et al.* constructed a nanodrug

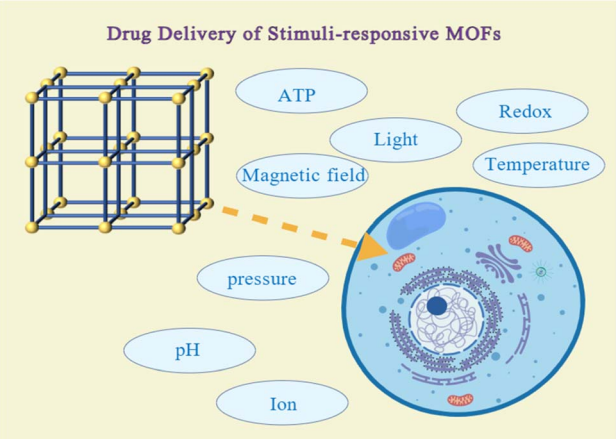

Fig. 12 MOFs with stimulus responsiveness.

delivery system with high stability and phosphate stimulation response.[166] The authors loaded cisplatin into the porous ZrMOFs and coated the surface with a cross-linked PAC polymer. After phosphate stimulation, the ZrMOFs etch, accelerating the release of the drug trapped in the ZrMOF–PAC nanoparticles. Therefore, Zr-based MOF is very sensitive to phosphate buffered saline. The polymeric coating of ZrMOFs enables ion-responsive MOFs to be both stable and physiologically stable for drug delivery. The temperature-responsive targeted drug delivery system can cause changes in physical and chemical properties according to the stimulation of ambient temperature to achieve controlled drug release. In general, this effect is achieved by ambient temperature modification and mainly depends on the supramolecular interaction between MOFs and other materials. Chen *et al.* encapsulated CP1@1 based on the polymers polyacrylamide (PAM) and polypyrrole (PPy) to form a smart nanodrug delivery system.[167] PAM–PPy can convert near-infrared (NIR) light energy into heat energy, and through the stimulation of temperature, achieve drug release. Compared with the explosive release, the release rate of PAM–PPy@CP1@1 regulated by temperature is more stable, so that the drug effect can be better played. This can be used as a reference for the construction of nano-drug delivery system for photothermal and photodynamic therapy. In the external stimulation, the triggering condition that deserves attention is the magnetic field. Due to their high magnetic behavior, magnetically responsive nanomaterials have been applied to construct nano-targeted delivery systems, and have played a positive role in magnetic resonance imaging (MRI), magnetic thermal therapy (MHT), magnetically responsive drug delivery, *etc.*, which have great potential in anti-tumor.[168] Magnetic nanomaterials (MNM) include nano-scale Fe-based magnetic metal dopants or alloys, such as Fe, Co, Ni, Mn, Gd, magnetic metal oxides and transition metal iron ore. Magnetically guided anticancer targeted drug delivery is a unique strategy to concentrate magnetic nano-targeted delivery systems at the tumor site through magnetic force to improve the therapeutic effect. Cao *et al.* constructed MOFS-based magnetic microrobot population (MMRS).[169] MMRS driven by magnetic fields play an important role in anti-tumor cells due to their precise control, good targeting and biological system compatibility. For the construction of MMRS, the authors chose the one-pot method to prepare magnetically inductive Fe@ZIF-8 nanoparticles with high loading of the anti-tumor drug Dox. The results showed that MMRS had a high drug loading capacity with a loading efficiency of 68.73%. In addition, MMRS also had good swarm configuration transformation: under the action of different magnetic fields, MMRS could show chained, vortex and oval swarms, and the movement direction of the swarms could be flexibly controlled by adjusting the yaw angle of the corresponding magnetic field. The vortex-like MMRSs can move along a predetermined trajectory, showing excellent control and adaptability. The construction of MMRS opens up a new way for accurate and non-invasive targeted drug delivery. Photosensitizers or PTCA have problems such as poor stability, transport efficiency, insufficient release, and breaking through the cellular microenvironment to reach tumor cells. Therefore, the construction of responsive MOFs materials can better solve the above problems, and the nano-sized drug delivery system can better transport *in vivo*.

6. Challenges and application prospects of MOFs in the treatment of tumor diseases

Due to their unique structural plasticity, MOFs have become one of the most promising material platforms in the field of PDT/PTT. Compared with some organic and inorganic materials, MOFs can be easily modified into nano-targeted delivery systems. The coating materials can simply be adsorbed from the aqueous medium to the surface of the MOF, resulting in high yield and good stability.[170] MOFs effectively solve the bottlenecks of traditional phototherapy drugs such as poor stability *in vivo*, easy quenching, damage to normal tissues, and limitation of hypoxia microenvironment. At the same time, MOFs support multimodal image-guided personalized treatment. By precisely regulating the pore size and surface functionalization of MOFs, the specific response of MOFs to different tumor microenvironments can be realized. For example, according to the hypoxic characteristics of tumor tissue, the design of MOFs with oxygen release function can significantly improve the therapeutic effect of PDT. Secondly, the integration of multimodal imaging and treatment is a key trend in the future development. The high specific surface area and structural plasticity of MOFs provide an ideal platform for loading a variety of functional molecules. By integrating fluorescence imaging, magnetic resonance imaging, and photoacoustic imaging, MOFs can not only achieve accurate tumor localization, but also monitor the treatment effect in real time.[171] This strategy of integrated diagnosis and treatment is expected to greatly improve the accuracy and safety of treatment. In addition, the exploration of combined treatment mode is also the focus of future research. MOFs can be loaded with photosensitizers and photothermal agents, and synergetic with chemotherapeutic drugs or immunomodulators. For example, the combined application of

MOFs-mediated PDT/PTT and immune checkpoint inhibitors may significantly inhibit tumor recurrence and metastasis by activating anti-tumor immune responses. This multi-mechanism synergistic treatment mode will bring new breakthroughs in tumor treatment.

Nano-targeted DDS constructed by MOFs have been applied from PTT or PDT therapy alone to combined application, but their clinical application still faces many challenges. Nowadays, the application of MOFs drugs is cautious and cautious. Most of the metals used in MOFs synthesis are non-degradable, so the well-known toxic metals such as lead, arsenic, chromium and cadmium will cause inevitable damage to the body of patients. Therefore, the proper selection of metal ions is very important for the construction of nano-targeted delivery system. Moreover, some solvents used to synthesize MOFs may remain in their pores. During the experiment, we can only use drying, freeze-drying and other methods to remove the solvents as much as possible, but certain side effects do occur when applied to patients. This requires us to choose the appropriate MOFs to improve the efficacy and safety of conventional disease therapies. At present, the synthesis process of MOFs is complex and costly, which limits its large-scale application. Future research should focus on the development of green and efficient synthesis methods, while strengthening the biocompatibility and long-term safety assessment of MOFs.

Future studies need to explore the safety, stability, targeting and clinical transformation of MOFs to promote the wide application of MOFs in tumor therapy.[172] Further optimization is needed for the large-scale production and clinical translation of MOFs. Through standardized production processes and rigorous toxicological studies, MOFs are expected to move from the laboratory to the clinic and become an important tool for cancer treatment. With the development of biomedicine, the preparation of safer, more effective and less side effects of MOFs nano-targeted delivery system will have a broad prospect.

7. Conclusion

MOFs, as a novel class of porous crystalline materials characterized by structural diversity and functional tunability, are emerging as a pivotal advancement in the field of cancer phototherapy, offering innovative solutions to the limitations in therapeutic efficacy and safety associated with conventional approaches. Their application in PDT, PTT and combined therapeutic modalities provides a substantial theoretical foundation and technical pathway for the development of efficient and low-toxicity nano-targeted DDS. With ongoing optimization of synthetic methodologies, enhanced biological safety profiles, and refined strategies for multimodal synergy, MOF-mediated phototherapy holds considerable promise for translation from laboratory research to clinical application, thereby enabling transformative progress in cancer treatment and positioning itself as a highly promising therapeutic strategy in the era of precision medicine.

Author contributions

Mengyu Xu: writing – original draft, visualization, investigation, data curation, conceptualization. Liyuan Wang: writing review & editing, Yuanxin Chen: writing review & editing, resources, conceptualization. Lihua Ma: writing – review & editing, conceptualization, Min Liu: writing – original draft, Long Wang: writing – original draft, resource. Jing Huan, Lijuan Wang and Yanxi Zhu: supervision, writing review & editing.

Conflicts of interest

The authors declare no conflicts of interest.

Data availability

No primary research results, software or code have been included and no new data were generated or analysed as part of this review.

Acknowledgements

The authors thank for the Funds for the Natural Science Foundation of Shandong Province (ZR2022MH058), Linyi City People's Hospital Science and Innovation Team: B-Cell Tumor Biology Leading Scientific Innovation Team Project (LYSRMYY-KCTD-001) and Shandong Province Traditional Chinese Medicine Science and Technology Development Plan (M20241201).

References

1 P. Saultier and G. Michel, *Blood*, 2024, **143**, 1795–1806.
2 L. Chen, Q. Wang, Y. Jiang, L. Xu, N. Wei, C. Lu, C. Chang, D. Song, Y. Wang, L. Wu, W. Li, X. Jia, K. Zhao, H. Hua, R. Chen and Z. Chen, *Chem. Eng. J.*, 2024, **496**, 154169.
3 C. S. Sia, B. T. Tey and L. E. Low, *Adv. Funct. Mater.*, 2024, **34**, 2314278.
4 L. Cheng, C. Wang, L. Feng, K. Yang and Z. Liu, *Chem. Rev.*, 2014, **114**, 10869–10939.
5 X. Li, X. Li, S. Park, S. Wu, Y. Guo, K. T. Nam, N. Kwon, J. Yoon and Q. Hu, *Coord. Chem. Rev.*, 2024, **520**, 216142.
6 Y. Du, J. Zhao, S. Li and H. Yuan, *Mol. Cancer*, 2025, **24**, 200.
7 H. Zhang, M. Cui, D. Tang, B. Wang, G. Liang, C. Xu and H. Xiao, *Adv. Mater.*, 2024, **36**, 2310298.
8 Z. Chen, Z. He, X. Li, Y. Wei, H. Xu, Y. Lin, X. Wei, Y. Huang, J. Hou, H. Wang and S. Li, *Adv. Funct. Mater.*, 2025, 2503055.
9 H. Yang, Q. Zhang, L. Dai, Y. Wang, G. Zheng, X. Zhang, D. Zheng, X. Ji, Y. Sang and Z. Nie, *Adv. Healthcare Mater.*, 2024, **13**, 2400662.
10 X. Pan, M. Hu, L. Wu, E. Wei, Q. Zhu, L. Lv, X. Xv, X. Dong, H. Liu and Y. Liu, *Adv. Sci.*, 2025, **12**, 2501722.
11 Y.-Q. Niu, J.-H. Liu, C. Aymonier, S. Fermani, D. Kralj, G. Falini and C.-H. Zhou, *Chem. Soc. Rev.*, 2022, **51**, 7883–7943.
12 Y. Guan, W. Zhang, Y. Mao and S. Li, *Mol. Cancer*, 2024, **23**, 246.

13 L. Fang, Z. Chen, J. Dai, Y. Pan, Y. Tu, Q. Meng, Y. Diao, S. Yang, W. Guo, L. Li, J. Liu, H. Wen, K. Hua, L. Hang, J. Fang, X. Meng, P. Ma and G. Jiang, *Adv. Sci.*, 2025, **12**, 2409157.
14 J. Li, Z. Yue, M. Tang, W. Wang, Y. Sun, T. Sun and C. Chen, *Adv. Healthcare Mater.*, 2023, **13**, 2302028.
15 F. Tang, A. Ding, Y. Xu, Y. Ye, L. Li, R. Xie and W. Huang, *Small*, 2023, **20**, 2307078.
16 C. Kong and X. Chen, *Int. J. Nanomed.*, 2022, **17**, 6427–6446.
17 Y. Xiong, Y. Rao, J. Hu, Z. Luo and C. Chen, *Adv. Mater.*, 2025, **37**, 2305140.
18 C. Chen, L. Shen, B. Wang, X. Lu, S. Raza, J. Xu, B. Li, H. Lin and B. Chen, *Chem. Soc. Rev.*, 2025, **54**, 2208–2245.
19 Z. Li, K. Xu, L. Qin, D. Zhao, N. Yang, D. Wang and Y. Yang, *Adv. Mater.*, 2023, **35**, 2203890.
20 B. Nasseri, E. Alizadeh, F. Bani, S. Davaran, A. Akbarzadeh, N. Rabiee, A. Bahadori, M. Ziaei, M. Bagherzadeh, M. R. Saeb, M. Mozafari and M. R. Hamblin, *Appl. Phys. Rev.*, 2022, **9**(1), 011317.
21 L. Sun, Y. Zhao, H. Peng, J. Zhou, Q. Zhang, J. Yan, Y. Liu, S. Guo, X. Wu and B. Li, *J. Nanobiotechnol.*, 2024, **22**, 210.
22 S. Liu, B. Wang, Y. Yu, Y. Liu, Z. Zhuang, Z. Zhao, G. Feng, A. Qin and B. Z. Tang, *ACS Nano*, 2022, **16**, 9130–9141.
23 M. Wang, H. Lai, Y. Gu, J. Yi, W. Wu, H. Li, S. Hou, L. Han, G. Fan, J. Huang, F. He and L. Tian, *Adv. Funct. Mater.*, 2025, e18174.
24 M. Yang, L. Zhou, Y.-Y. Zhao, K. M. K. Swamy, A. Chen and J. Yoon, *Sci. Bull.*, 2025, **70**, 1203–1206.
25 D. Huang, H. Huang, M. Li, J. Fan, W. Sun, J. Du, S. Long and X. Peng, *Adv. Funct. Mater.*, 2022, **32**, 2208105.
26 Q. Zhang, Y. Li, C. Jiang, W. Sun, J. Tao and L. Lu, *Adv. Healthcare Mater.*, 2023, **12**, 2301502.
27 S. Kwon, H. Ko, D. G. You, K. Kataoka and J. H. Park, *Acc. Chem. Res.*, 2019, **52**, 1771–1782.
28 M. Li, Y. Xu, X. Peng and J. S. Kim, *Acc. Chem. Res.*, 2022, **55**, 3253–3264.
29 V. F. Otvagin, N. S. Kuzmina, E. S. Kudriashova, A. V. Nyuchev, A. E. Gavryushin and A. Y. Fedorov, *J. Med. Chem.*, 2022, **65**, 1695–1734.
30 E. V. D. Luca, S. Tambone, S. Catapano, B. Fossati and K. Peris, *Dermatol. Ther.*, 2020, **33**, e14518.
31 A. Juzeniene and J. Moan, *Photodiagn. Photodyn. Ther.*, 2007, **4**, 80–87.
32 J. Karges, *Angew. Chem., Int. Ed.*, 2021, **61**, e202112236.
33 D. A. Siriwardane, W. Jiang and T. Mudalige, *Int. J. Pharm.*, 2023, **646**, 123449.
34 M. Kuwatani and N. Sakamoto, *Cancers*, 2023, **15**, 3686.
35 A. Wiehe and M. O. Senge, *Photochem. Photobiol.*, 2022, **99**, 356–419.
36 J. M. Dąbrowski and L. G. Arnaut, *Photochem. Photobiol. Sci.*, 2015, **14**, 1765–1780.
37 N. Mehan, M. Kumar, S. Bhatt, R. Shankar, B. Kumari, R. Pahwa and D. Kaushik, *Crit. Rev. Ther. Drug Carrier Syst.*, 2022, **39**, 79–95.
38 S. Kishimoto, M. Bernardo, K. Saito, S. Koyasu, J. B. Mitchell, P. L. Choyke and M. C. Krishna, *Free Radical Biol. Med.*, 2015, **85**, 24–32.
39 D. E. Dolmans, D. Fukumura and R. K. Jain, *Nat. Rev. Cancer*, 2003, **3**, 380–387.
40 J. P. Celli, B. Q. Spring, I. Rizvi, C. L. Evans, K. S. Samkoe, S. Verma, B. W. Pogue and T. Hasan, *Chem. Rev.*, 2010, **110**, 2795–2838.
41 W. Jiang, M. Liang, Q. Lei, G. Li and S. Wu, *Cancers*, 2023, **15**, 585.
42 M. Zhang, Y. Zhao, H. Ma, Y. Sun and J. Cao, *Theranostics*, 2022, **12**, 4629–4655.
43 A. Escudero, C. Carrillo-Carrión, M. C. Castillejos, E. Romero-Ben, C. Rosales-Barrios and N. Khiar, *Mater. Chem. Front.*, 2021, **5**, 3788–3812.
44 M. Orfano, J. Perego, C. X. Bezuidenhout, I. Villa, R. Lorenzi, B. Sabot, S. Pierre, S. Bracco, S. Piva, A. Comotti and A. Monguzzi, *Adv. Funct. Mater.*, 2024, **34**, 2404480.
45 C. Xu and K. Pu, *Chem. Soc. Rev.*, 2021, **50**, 1111–1137.
46 Y. Hang, A. Wang and N. Wu, *Chem. Soc. Rev.*, 2024, **53**, 2932–2971.
47 H. S. Han and K. Y. Choi, *Biomedicines*, 2021, **9**, 305.
48 Z. Bai, L. Zhao, Z. Xin, J. Li, Y. Bai and F. Feng, *Mol. Pharmaceutics*, 2025, **22**, 4995–5006.
49 N. Li, Y. Wang, Y. Li, C. Zhang and G. Fang, *Small*, 2024, **20**, 2305645.
50 H.-G. Jin, P.-C. Zhao, Y. Qian, J.-D. Xiao, Z.-S. Chao and H.-L. Jiang, *Chem. Soc. Rev.*, 2024, **53**, 9378–9418.
51 X.-L. Weng and J.-Y. Liu, *Drug Discovery Today*, 2021, **26**, 2045–2052.
52 C. Du, X. Wu, M. He, Y. Zhang, R. Zhang and C.-M. Dong, *J. Mater. Chem. B*, 2021, **9**, 1478–1490.
53 L. Tian, X. Li, H. Ji, Q. Yu, M. Yang, L. Guo, L. Huang and W. Gao, *J. Nanobiotechnol.*, 2022, **20**, 485.
54 Q. Chen, L. Xu, C. Liang, C. Wang, R. Peng and Z. Liu, *Nat. Commun.*, 2016, **7**, 13193.
55 M. Overchuk, R. A. Weersink, B. C. Wilson and G. Zheng, *ACS Nano*, 2023, **17**, 7979–8003.
56 S. R. Dash and C. N. Kundu, *Curr. Nanosci.*, 2022, **18**, 31–47.
57 W. Zhang, X. Ding, H. Cheng, C. Yin, J. Yan, Z. Mou, W. Wang, D. Cui, C. Fan and D. Sun, *Theranostics*, 2023, **13**, 2964.
58 M. Li, H. Jiang, P. Hu and J. Shi, *Angew. Chem.*, 2024, **136**, e202316606.
59 Y. Zhang, J. Li and K. Pu, *Biomaterials*, 2022, **291**, 121906.
60 R.-L. Ge, P.-N. Yan, Y. Liu, Z.-S. Li, S.-Q. Shen and Y. Yu, *Adv. Funct. Mater.*, 2023, **33**, 2301138.
61 Q. Fu, R. Zhu, J. Song, H. Yang and X. Chen, *Adv. Mater.*, 2019, **31**, 1805875.
62 S. Yuan, L. Feng, K. Wang, J. Pang, M. Bosch, C. Lollar, Y. Sun, J. Qin, X. Yang, P. Zhang, Q. Wang, L. Zou, Y. Zhang, L. Zhang, Y. Fang, J. Li and H.-C. Zhou, *Adv. Mater.*, 2018, **30**, 1704303.
63 M. Yang, C. Ji and M. Yin, *Wiley Interdiscip. Rev.:Nanomed. Nanobiotechnol.*, 2024, **16**, e1960.
64 N. Beniwal, A. Verma, C. L. Putta and A. K. Rengan, *Nanotheranostics*, 2024, **8**, 219–238.

65 K. Li, K. Xu, S. Liu, Y. He, M. Tan, Y. Mao, Y. Yang, J. Wu, Q. Feng, Z. Luo and K. Cai, *ACS Nano*, 2023, **17**, 20218–20236.
66 F. Liang, D. Ma, L. Qin, Q. Yu, J. Chen, R. Liang, C. Zhong, H. Liao and Z. Peng, *Dalton Trans.*, 2024, **53**, 10070–10074.
67 E. Tomic, *J. Appl. Polym. Sci.*, 1965, **9**, 3745–3752.
68 B. F. Hoskins and R. Robson, *J. Am. Chem. Soc.*, 1990, **112**, 1546–1554.
69 O. M. Yaghi, G. Li and H. Li, *Nature*, 1995, **378**, 703–706.
70 M. Kondo, T. Yoshitomi, H. Matsuzaka, S. Kitagawa and K. Seki, *Angew. Chem., Int. Ed. Engl.*, 1997, **36**, 1725–1727.
71 H. Li, M. Eddaoudi, M. O'Keeffe and O. M. Yaghi, *Nature*, 1999, **402**, 276–279.
72 L. Qin, Y. Li, D. Ma, F. Liang, L. Chen, C. Xie, J. Lin, Y. Pan, G. Li, F. Chen, P. Xu, C. Hong and J. Zhu, *J. Solid State Chem.*, 2022, **312**, 123175.
73 M. Koshy, M. Spiotto, L. E. Feldman, J. J. Luke, G. F. Fleming, D. Olson, J. W. Moroney, R. Nanda, A. Rosenberg, A. T. Pearson, A. Juloori, F. Weinberg, C. Ray, R. C. Gaba, P. J. Chang, L. A. Janisch, Z.-Q. Xu, W. Lin, R. R. Weichselbaum and S. J. Chmura, *J. Clin. Oncol.*, 2023, **41**, 2527.
74 G. Chen, G. Liu, Y. Pan, G. Liu, X. Gu, W. Jin and N. Xu, *Chem. Soc. Rev.*, 2023, **52**, 4586–4602.
75 S. He, L. Wu, X. Li, H. Sun, T. Xiong, J. Liu, C. Huang, H. Xu, H. Sun and W. Chen, *Acta Pharm. Sin. B*, 2021, **11**, 2362–2395.
76 A. E. Nel, W. J. Parak, W. C. Chan, T. Xia, M. C. Hersam, C. J. Brinker, J. I. Zink, K. E. Pinkerton, D. R. Baer and P. S. Weiss, *ACS Nano*, 2015, **9**, 5627–5630.
77 R. Ettlinger, U. Lächelt, R. Gref, P. Horcajada, T. Lammers, C. Serre, P. Couvreur, R. E. Morris and S. Wuttke, *Chem. Soc. Rev.*, 2022, **51**, 464–484.
78 P. Horcajada, R. Gref, T. Baati, P. K. Allan, G. Maurin, P. Couvreur, G. Férey, R. E. Morris and C. Serre, *Chem. Rev.*, 2012, **112**, 1232–1268.
79 L. Dongmei, W. Zhiwei, Z. Qi, C. Fuyi, S. Yujuan and L. Xiaodong, *Regul. Toxicol. Pharmacol.*, 2015, **73**, 802–810.
80 G. Férey, C. Serre, C. Mellot-Draznieks, F. Millange, S. Surblé, J. Dutour and I. Margiolaki, *Angew. Chem.*, 2004, **116**, 6456–6461.
81 S.-H. Jhung, J.-H. Lee and J.-S. Chang, *Bull. Korean Chem. Soc.*, 2005, **26**, 880–881.
82 G. Ferey, *Science*, 2005, **309**, 2040–2042.
83 L. Oar-Arteta, T. Wezendonk, X. Sun, F. Kapteijn and J. Gascon, *Mater. Chem. Front.*, 2017, **1**, 1709–1745.
84 H. Yang, F. Peng, A. N. Hong, Y. Wang, X. Bu and P. Feng, *J. Am. Chem. Soc.*, 2021, **143**, 14470–14474.
85 T. Pan, Y. Wang, F. Liu, C. Liu and W. Li, *J. Solid State Chem.*, 2022, **306**, 122732.
86 C. J. Wijaya, S. Ismadji, H. W. Aparamarta and S. Gunawan, *Molecules*, 2021, **26**, 6430.
87 L. Liang, C. Liu, F. Jiang, Q. Chen, L. Zhang, H. Xue, H.-L. Jiang, J. Qian, D. Yuan and M. Hong, *Nat. Commun.*, 2017, **8**, 1233.
88 B. Abdollahi, M. Zarei and D. Salari, *J. Solid State Chem.*, 2022, **311**, 123132.
89 B. Yang, M. Shao, Y. Xu, Y. Du, H. Yang, D. Bin, B. Liu and H. Lu, *ChemElectroChem*, 2022, **9**, e202200438.
90 P. Horcajada, C. Serre, G. Maurin, N. A. Ramsahye, F. Balas, M. Vallet-Regí, M. Sebban, F. Taulelle and G. Férey, *J. Am. Chem. Soc.*, 2008, **130**, 6774–6780.
91 A. V. Neimark, F.-X. Coudert, A. Boutin and A. H. Fuchs, *J. Phys. Chem. Lett.*, 2010, **1**, 445–449.
92 P. Horcajada, C. Serre, M. Vallet-Regí, M. Sebban, F. Taulelle and G. Férey, *Angew. Chem., Int. Ed.*, 2006, **45**, 5974–5978.
93 T. Zhang, Z. Jiang, L. Chen, C. Pan, S. Sun, C. Liu, Z. Li, W. Ren, A. Wu and P. Huang, *Nano Res.*, 2020, **13**, 273–281.
94 J. H. Cavka, S. Jakobsen, U. Olsbye, N. Guillou, C. Lamberti, S. Bordiga and K. P. Lillerud, *J. Am. Chem. Soc.*, 2008, **130**, 13850–13851.
95 A. Schaate, P. Roy, A. Godt, J. Lippke, F. Waltz, M. Wiebcke and P. Behrens, *Chem.–Eur. J.*, 2011, **17**, 6643–6651.
96 M. Zhang, Y. Chen, M. Bosch, T. Gentle III, K. Wang, D. Feng, Z. U. Wang and H. Zhou, *Angew. Chem.*, 2014, **126**, 834–837.
97 K. Chattopadhyay, M. Mandal and D. K. Maiti, *Mater. Adv.*, 2024, **5**, 51–67.
98 S. S.-Y. Chui, S. M.-F. Lo, J. P. Charmant, A. G. Orpen and I. D. Williams, *Science*, 1999, **283**, 1148–1150.
99 V. M. V and G. Nageswaran, *J. Electrochem. Soc.*, 2020, **167**, 155527.
100 X. Wang, M. Zhou, Y. Liu and Z. Si, *Cancer Lett.*, 2023, **561**, 216157.
101 H. Li, M. Eddaoudi, T. L. Groy and O. Yaghi, *J. Am. Chem. Soc.*, 1998, **120**, 8571–8572.
102 K. S. Park, Z. Ni, A. P. Côté, J. Y. Choi, R. Huang, F. J. Uribe-Romo, H. K. Chae, M. O'Keeffe and O. M. Yaghi, *Proc. Natl. Acad. Sci. U. S. A.*, 2006, **103**, 10186–10191.
103 Y. Pan, Y. Liu, G. Zeng, L. Zhao and Z. Lai, *Chem. Commun.*, 2011, **47**, 2071–2073.
104 T. He, X. Xu, B. Ni, H. Wang, Y. Long, W. Hu and X. Wang, *Nanoscale*, 2017, **9**, 19209–19215.
105 S. Rojas-Buzo, C. Pontremoli, S. De Toni, K. Bondar, S. Galliano, H. Paja, B. Civalleri, A. Fiorio Pla, C. Barolo, F. Bonino and N. Barbero, *ACS Appl. Mater. Interfaces*, 2025, **17**, 524–536.
106 Y. Shao, M. Chen, W. Chen, Z. Wang, M. Sui, M. Tian, Y. Wu, J. Song, D. Ji and F. Song, *Adv. Healthcare Mater.*, 2023, **12**(25), 2300503.
107 X. Zhao, J. Liu, J. Fan, H. Chao and X. Peng, *Chem. Soc. Rev.*, 2021, **50**, 4185–4219.
108 W. M. Darwish, N. A. Bayoumi, H. M. El-Shershaby and N. M. Allahloubi, *J. Photochem. Photobiol., B*, 2020, **203**, 111777.
109 X. Zhao, Z. Chen, S. Zhang, Z. Hu, J. Shan, M. Wang, X.-L. Chen and X. Wang, *J. Nanobiotechnol.*, 2024, **22**(1), 387.
110 G. Lan, K. Ni and W. Lin, *Coord. Chem. Rev.*, 2019, **379**, 65–81.
111 K. Lu, C. He and W. Lin, *J. Am. Chem. Soc.*, 2014, **136**, 16712–16715.

112 D. Zhao, W. Zhang, S. Yu, S.-L. Xia, Y.-N. Liu and G.-J. Yang, *J. Nanobiotechnol.*, 2022, **20**, 421.
113 R. Dai, F. Peng, P. Ji, K. Lu, C. Wang, J. Sun and W. Lin, *Inorg. Chem.*, 2017, **56**, 8128–8134.
114 K. Lu, C. He and W. Lin, *J. Am. Chem. Soc.*, 2015, **137**, 7600–7603.
115 Y. Ma, X. Li, A. Li, P. Yang, C. Zhang and B. Tang, *Angew. Chem., Int. Ed.*, 2017, **56**, 13752–13756.
116 B. Liu, Z. Liu, X. Lu, P. Wu, Z. Sun, H. Chu and H. Peng, *Mater. Des.*, 2023, **228**, 111861.
117 Z. Shi, K. Zhang, S. Zada, C. Zhang, X. Meng, Z. Yang and H. Dong, *ACS Appl. Mater. Interfaces*, 2020, **12**, 12600–12608.
118 W. Zhang, J. Lu, X. Gao, P. Li, W. Zhang, Y. Ma, H. Wang and B. Tang, *Angew. Chem., Int. Ed.*, 2018, **57**, 4891–4896.
119 G. Lan, K. Ni, S. S. Veroneau, X. Feng, G. T. Nash, T. Luo, Z. Xu and W. Lin, *J. Am. Chem. Soc.*, 2019, **141**, 4204–4208.
120 Y. Wan, L.-H. Fu, C. Li, J. Lin and P. Huang, *Adv. Mater.*, 2021, **33**, 2103978.
121 Y. Xuan, M. Guan and S. Zhang, *Theranostics*, 2021, **11**, 7360–7378.
122 J. Chen, X. Tan, Y. Huang, C. Xu, Z. Zeng, T. Shan, Z. Guan, X. Xu, Z. Huang and C. Zhao, *Biomaterials*, 2022, **284**, 121513.
123 X. Cheng, H.-D. Xu, H.-H. Ran, G. Liang and F.-G. Wu, *ACS Nano*, 2021, **15**, 8039–8068.
124 M. Liu, H. Wu, S. Wang, J. Hu and B. Sun, *J. Mater. Chem. B*, 2021, **9**, 9413–9422.
125 Y. Chen, Y. Chen, Z. Wang, L. Yang, Y. Zhang, Z. Zhang and L. Jia, *J. Nanobiotechnol.*, 2024, **22**, 705.
126 Y. Chu, X.-Q. Xu and Y. Wang, *J. Phys. Chem. Lett.*, 2022, **13**, 9564–9572.
127 D. W. Thuita and C. Brückner, *Chem. Rev.*, 2022, **122**, 7990–8052.
128 J. M. Park, K.-I. Hong, H. Lee and W.-D. Jang, *Acc. Chem. Res.*, 2021, **54**, 2249–2260.
129 J. Chen, Y. Zhu and S. Kaskel, *Angew. Chem., Int. Ed.*, 2020, **60**, 5010–5035.
130 D. Xu, Q. Duan, H. Yu and W. Dong, *J. Mater. Chem. B*, 2023, **11**, 5976–5989.
131 Z. Wang, Q. Sun, B. Liu, Y. Kuang, A. Gulzar, F. He, S. Gai, P. Yang and J. Lin, *Coord. Chem. Rev.*, 2021, **439**, 213945.
132 K. Zhang, X. Meng, Y. Cao, Z. Yang, H. Dong, Y. Zhang, H. Lu, Z. Shi and X. Zhang, *Adv. Funct. Mater.*, 2018, **28**, 1804634.
133 X. Cui, Q. Ruan, X. Zhuo, X. Xia, J. Hu, R. Fu, Y. Li, J. Wang and H. Xu, *Chem. Rev.*, 2023, **123**, 6891–6952.
134 B. Lü, Y. Chen, P. Li, B. Wang, K. Müllen and M. Yin, *Nat. Commun.*, 2019, **10**, 767.
135 Z. Deng, C. Fang, X. Ma, X. Li, Y.-J. Zeng and X. Peng, *ACS Appl. Mater. Interfaces*, 2020, **12**, 20321–20330.
136 W. Pan, Z. Li, S. Qiu, C. Dai, S. Wu, X. Zheng, M. Guan and F. Gao, *Mater. Today Bio*, 2022, **13**, 100214.
137 J.-Y. Zeng, M.-K. Zhang, M.-Y. Peng, D. Gong and X.-Z. Zhang, *Adv. Funct. Mater.*, 2018, **28**, 1705451.
138 S. T. Nejad, R. Rahimi, M. Najafi and S. Rostamnia, *ACS Appl. Mater. Interfaces*, 2024, **16**, 3162–3170.
139 D. E. Large, J. R. Soucy, J. Hebert and D. T. Auguste, *Adv. Ther.*, 2019, **2**, 1800091.
140 W.-C. Chien, P.-H. Cheng, X.-J. Cheng, C.-C. Chuang, Y.-T. Huang, T. S. Anilkumar, C.-H. Liu, Y.-J. Lu and K. C.-W. Wu, *ACS Appl. Mater. Interfaces*, 2021, **13**, 52092–52105.
141 W. Wang, L. Wang, Y. Li, S. Liu, Z. Xie and X. Jing, *Adv. Mater.*, 2016, **28**, 9320–9325.
142 W. Wang, L. Wang, S. Liu and Z. Xie, *Bioconjugate Chem.*, 2017, **28**, 2784–2793.
143 B. Yang, H. Fu, R. Kong, G. Zheng, X. Wang, Y. Dong and Z. Yang, *J. Mater. Chem. B*, 2022, **10**, 8490–8501.
144 L. Huang, Y. Luo, Y. Cong, J. Liu, C. Xu, Z. Zeng, Y. Yin, H. Hong and W. Xu, *New J. Chem.*, 2024, **48**, 8773–8788.
145 M. Ding, W. Liu and R. Gref, *Adv. Drug Delivery Rev.*, 2022, **190**, 114496.
146 G. Lan, K. Ni, Z. Xu, S. S. Veroneau, Y. Song and W. Lin, *J. Am. Chem. Soc.*, 2018, **140**, 5670–5673.
147 B. Liu, H. Zhou, L. Tan, K. T. H. Siu and X.-Y. Guan, *Signal Transduction Targeted Ther.*, 2024, **9**, 175.
148 Z. Liang, X. Li, X. Chen, J. Zhou, Y. Li, J. Peng, Z. Lin, G. Liu, X. Zeng, C. Li, L. Hang and H. Li, *Front. Bioeng. Biotechnol.*, 2023, **11**, 1156079.
149 X. Lin, H. Wu, J. Zhang, X. Chen, X. Gao and Y. Liu, *Chem. Eng. J.*, 2024, **480**, 147865.
150 L. Wang, X. Qu, Y. Zhao, Y. Weng, G. I. N. Waterhouse, H. Yan, S. Guan and S. Zhou, *ACS Appl. Mater. Interfaces*, 2019, **11**, 35228–35237.
151 X. Cai, Y. Zhao, L. Wang, M. Hu, Z. Wu, L. Liu, W. Zhu and R. Pei, *J. Mater. Chem. B*, 2021, **9**, 6646–6657.
152 B. Liu, X. Liu, X. Zhang, X. Wu, C. Li, Z. Sun and H. Chu, *Cancer Nanotechnol.*, 2022, **13**, 18.
153 G. Gao, J. Che, P. Xu, B. Chen and Y. Zhao, *Aggregate*, 2024, **5**, e631.
154 T. Mamo, E. A. Moseman, N. Kolishetti, C. Salvador-Morales, J. Shi, D. R. Kuritzkes, R. Langer, U. V. Andrian and O. C. Farokhzad, *Nanomed*, 2010, **5**, 269–285.
155 A. Z. Mirza and F. A. Siddiqui, *Int. Nano Lett.*, 2014, **4**, 94.
156 W. Deng, Z. Wei, Y. Xu, Z. Gong, F. Cai, Q. Shi, K. Guo, M. Jia, Y. Zhao, Y. Feng, J. Deng and B. Zhang, *Small*, 2025, **21**, 2408975.
157 Y. Yang, Y. Chao, J. Liu, Z. Dong, W. He, R. Zhang, K. Yang, M. Chen and Z. Liu, *NPG Asia Mater.*, 2017, **9**, e344.
158 B. Li, X. Wang, L. Chen, Y. Zhou, W. Dang, J. Chang and C. Wu, *Theranostics*, 2018, **8**, 4086–4096.
159 Y. Cheng, C. Wen, Y.-Q. Sun, H. Yu and X.-B. Yin, *Adv. Funct. Mater.*, 2021, **31**(37), 2104378.
160 S. F. Fatima, R. Sabouni, R. Garg and H. Gomaa, *Colloids Surf., B*, 2023, **225**, 113266.
161 Y. Shi, Y. Zhang, L. Zhu, Y. Miao, Y. Zhu and B. Yue, *Adv. Healthcare Mater.*, 2024, **13**, 2301726.
162 T. Wen, G. Quan, B. Niu, Y. Zhou, Y. Zhao, C. Lu, X. Pan and C. Wu, *Small*, 2021, **17**, 2005064.
163 X. Jing, H. Hu, Y. Sun, B. Yu, H. Cong and Y. Shen, *Small Methods*, 2022, **6**, 2101437.
164 Z. Guo, Y. Xiao, W. Wu, M. Zhe, P. Yu, S. Shakya, Z. Li and F. Xing, *J. Nanobiotechnol.*, 2025, **23**, 157.

165 S. Wu, S. Hu and X. Yang, *Front. Bioeng. Biotechnol.*, 2022, 945148.
166 Y. Liu, C. S. Gong, Y. Dai, Z. Yang, G. Yu, Y. Liu, M. Zhang, L. Lin, W. Tang, Z. Zhou, G. Zhu, J. Chen, O. Jacobson, D. O. Kiesewetter, Z. Wang and X. Chen, *Biomaterials*, 2019, **218**, 119365.
167 T. Chen, Y. Xiao and G. Fang, *J. Inorg. Organomet. Polym. Mater.*, 2025, **35**, 2456–2465.
168 Y. Yuan, B. Chen, L. Song, X. An, Q. Zhang, H. Lu, C. M. Li and C. Guo, *J. Mater. Chem. B*, 2024, **12**, 1404–1428.
169 Q. Cao, Y. Zhang, Y. Tang, C. Wu, J. Wang and D. Li, *Sci. China: Chem.*, 2024, **67**, 1216–1223.
170 J. Zhang, F. Wang, Z. Sun, J. Ye and H. Chu, *J. Nanobiotechnol.*, 2025, **23**, 161.
171 F. Liang, L. Qin, J. Xu, S. Li, C. Luo, H. Huang, D. Ma, Z. Li and J. Xu, *J. Solid State Chem.*, 2020, **289**, 121544.
172 J. Wang, D. Ma, W. Liao, S. Li, M. Huang, H. Liu, Y. Wang, R. Xie and J. Xu, *CrystEngComm*, 2017, **19**, 5244–5250.